Environmental drivers of spatio-temporal dynamics in floodplain vegetation: grasslands as habitat for megafauna in Bardia National Park (Nepal)

Jitse Bijlmakers[1], Jasper Griffioen[2,3] & Derek Karssenberg[1]

[1]Department of Physical Geography, Faculty of Geosciences, Utrecht University, the Netherlands
[2]Copernicus Institute of Sustainable Development, Faculty of Geosciences, Utrecht University, the Netherlands
[3]TNO Geological Survey of the Netherland, Utrecht, the Netherlands

Correspondence to: Jitse Bijlmakers (jitsebijl@xs4all.nl)

Abstract: Disturbance-dependent grasslands, often associated with hydromorphological and fire dynamics, are threatened, especially in subtropical climates. In the Nepalese and Indian Terai Arc Landscape at the foot of the Himalayas, natural and cultural grasslands serve a viable role for greater one-horned rhinoceros (*Rhinoceros unicornis*) and for grazers which form prey of the Royal Bengal tiger (*Panthera tigris*). The grasslands are vulnerable to encroachment of forest. We aimed to establish the effects of environmental drivers, in particular river discharge, river channel dynamics, precipitation, and forest fires, on the spatio-temporal dynamics of these grasslands. The study area is the floodplain of the eastern branch of the Karnali River and adjacent western part of Bardia National Park. We created annual time series (1993-2019) of land cover with the use of field data, remotely sensed LANDSAT imagery and a supervised classification model. Additionally, we analysed the pattern of grassland patches and aerial photographs of 1964. Between 1964 and 2019, grassland patches decreased in abundance and size due to encroachment of forest. Outside the floodplain, conversion of grassland to bare substrate coincides with extreme precipitation events. Within the floodplain, conversion of grassland to bare substrate correlates with the magnitude of the annual peak discharge of the bifurcated Karnali River. Since 2009, however, this correlation is absent due to a shift of the main discharge channel to the western branch of the Karnali River. Consequently, alluvial tall grasslands (*Saccharum spontaneum* dominant) have vastly expanded between 2009 and 2019. Because the hydromorphological processes in the floodplain have become more static, other sources of disturbances – local flooding of ephemeral streams, anthropogenic maintenance, grazing and fires – are more paramount to prevent encroachment of grasslands. Altogether, our findings underscore that a change in the environmental drivers impact the surface area and heterogeneity of grassland patches in the landscape, which can lead to cascading effects for the grassland-dependent megafauna.

1. Introduction

Grasslands occur in diverse environmental conditions that can be dry, wet, hot, cold, productive, barren, dynamic and static (Brown and Makings, 2014). Their global areal extent has decreased by 40% since the Industrial Era (White et al., 2000) due to cultivation, urbanisation and increased forest growth, causing loss of biodiversity (White et al., 2000; Veldman et al., 2015). Grasslands are home to most of the extant mammalian megafauna on Earth and provide food for herbivores, which in turn sustain their predators. This is for example the case in the African (sub)tropical grasslands as well as in the mountainous and colder grassland habitats in Mongolia and Nepal. Here, grassland-dependent blue sheep (*Pseudois nayaur*), Siberian ibex (*Capra sibirica*) and Tibetan argali *(Ovis ammon)* serve as principle prey species of the snow leopard (*Panthera unica*) and Himalayan wolf (*Canis lupus chanco*) (Oli, 1996; Lyngdoh et al., 2014; Chetri et al., 2017; Rovero et al., 2020; Filla et al., 2021). At the foot of mountain ranges, warmer and wetter conditions are present due to lower altitudes and orographic lift of

seasonal moist winds, causing the constraints for forest growth to be lifted (Staver et al., 2011; Hirota et al., 2011). The relationship between prey, predator and grassland habitat is also present in these regions more suited for forest growth: grassland patches in forests at the foot of mountainous regions in South Asia sustain Royal Bengal tigers (*Panthera tigris*) and their prey. This is for example the case in the Western Gaths, South India (Sankaran, 2009), in the Duars, Eastern India and Bhutan, and in the Terai Arc Landscape (TAL), a subtropical belt at the foot of the Indian and Nepalese Himalayas (Harihar et al., 2014, Irengbam et al., 2017a). Also the TAL has seen a reduction of grassland in protected areas (Irengbam et al., 2017).

Grasslands in the TAL can broadly be subdivided into (1) natural alluvial tall grassland, located near active and in abandoned river channels, and (2) a mosaic of short grassland (phantas) and mixed tall grassland, located further away from the river channels. The alluvial tall grasslands serve as essential habitat for the greater one-horned rhino (*Rhinoceros unicornis*) and hog deer (*Hyelaphus porcinus*) (Jnawali and Wegge, 2000; Odden et al., 2005; Pradhan et al., 2008; Thapa et al., 2013; DNPWC and DFSC, 2018) and their numbers would be greatly affected if changes occur in composition and areal extent of these grasslands (Odden et al., 2005; Peet, 1997). Tiger density is highest near grasslands and particularly the short grasslands provide nutritious feeding grounds for Chital deer (*Axis axis*), the most important prey (Moe and Wegge, 1994; DNPWC and DFSC, 2018). In addition to the surface area, the spatial pattern of grassland in the landscape is of importance: habitat heterogeneity is positively correlated with the abundance and habitat preference of Chital deer in the National Park of Chitwan (Nepal) (Bhattarai and Kindlmann, 2012).

A number of grasslands in the TAL are considered to be maintained via physical disturbances that prevent succession to mature vegetational stages (Seidensticker, 1976; Dinerstein, 1979a; Lehmkuhl, 1989, 1994; Peet et al., 1999b). In general, the pattern of vegetation is regulated by autogenic and allogenic factors (Tilman, 1988), of which the latter are either environmental or anthropogenic. Allogenically, the community dynamics can be controlled via disturbances, of which the intensity and spatial extent have been identified as principal factors (Turner et al., 1998). The natural disturbances recorded in the TAL include hydromorphological processes, fires, climatic variables (precipitation, temperature, droughts) and herbivory, whereas the anthropogenic disturbances include cutting of grasses and trees for maintenance and resource collection, clearance by fires, livestock grazing, and, in the past, cultivation and creation of settlements (Seidensticker, 1976; Dinerstein, 1979a; Lehmkuhl, 1989, 1994). Changes in disturbance regimes impact other disturbance regimes (Van Langevelde et al., 2003; Trauernicht et al., 2013; Orem and Pelletier, 2015), the vegetation pattern, and thus the ecosystem as a whole (Parr et al., 2012). Conversion of disturbance-dependent grassland to forest can occur within several years when changes occur in rainfall, fire or herbivory (Bond, 2008). In Bardia National Park (BNP), a conservation area in the TAL located near the Karnali megafan in Western Nepal, grasslands have been declining due to encroachment of forest (Peet et al., 1999a; Jnawali and Wegge, 2000; Odden, 2007). From a hydrological perspective, there are indications that a major change occurred during the monsoon in 2009 (Sinclair et al., 2017): near the apex of the highly dynamic braided river system of the Karnali River, the dominant discharge channel relocated from its eastern branch (the Geruwa River that borders BNP) to the western branch (Kauriala River). The susceptibility of land cover to changes in disturbance regimes not only holds for the grasslands in the TAL but also for other ecosystems where climate is conductive for forest growth. In the Brazilian Pantanal, where similar grasslands are found at the foot of the Brazilian Highlands, extreme hydrologic conditions have been explicitly identified with remote sensing as a driving factor of the pattern of vegetation communities (Arieira et al., 2011). The Taquari megafan in the Pantanal experienced a shift in hydrological conditions due to an avulsion, increasing susceptibility to deforestation and fire (Louzada et al., 2020).

Wide-ranging progress has been made in understanding the drivers of vegetation dynamics through space and time (Hupp and Osterkamp, 1996; Lorenz et al., 1997; Vesipa et al., 2017; Corenblit et al., 2007; Turner et al., 1998). The composition and spatial distribution of riparian vegetation communities are heavily influenced by flood frequency, duration, intensity (Hupp and Osterkamp, 1996; Poff et al., 1997) and timing (Newbold and Mountford, 1997). Consequences of high discharges for vegetation can be physical damage and uprooting, anoxia due to prolonged inundation, and burial by fresh alluvium. Low discharges affect vegetation with drought stress when the ground water table becomes too deep. These processes are integrated in concepts such as 'fluvial biogeomorphic succession', describing the reciprocal interactions between fluvial landforms and vegetation (Gunderson, 2002; Corenblit et al., 2007), 'flood pulse concept', describing lateral connectivity and recognizing that flow and its variability are the main drivers of ecological processes in floodplains (Junk et al., 1989), and 'shifting-mosaic steady state' for vegetation, which specifies on the proportion of distinct successional land cover in floodplains (Arscott et al., 2002; Kollmann et al., 1999). Additionally, fire dynamics (Flannigan and Wotton, 2001; Hoetzel et al., 2013; Iglesias et al., 2014), herbivory (Owen-Smith, 1988; Van Langevelde et al., 2003; Allred et al., 2011) as well as anthropogenic interferences (Wang et al., 2015) have been studied. The interrelations of environmental drivers are complex (Lehmann et al., 2014) and there is not yet a complete understanding. It is, therefore, of interest to study vegetation and its drivers at a high temporal resolution over a long time span and in its historic context. Literature in this domain is particularly limited to a small number of geographic regions (Dufour et al., 2019) and the subtropical grasslands in conservation areas in the TAL such as BNP are underrepresented. It is especially vital to understand the functioning of such a valuable ecosystem in relation to possible changes in drivers (such as the indicated redistribution of discharge in 2009) in order to provide insight for nature management strategies.

A promising method for studying land cover dynamics and its drivers is the use of earth observation techniques, which enable diachronic analysis (Lallias-Tacon et al., 2017; Dufour et al., 2019; Harezlak et al., 2020; Solins et al., 2017; Basumatary et al., 2021; Louzada et al., 2020; Van Iersel, 2020; Corenblit et al., 2010; Dufour et al., 2015). Vegetation in and near floodplains can be mapped at the following scales and characteristics: type (Alaibakhsh et al., 2017), species composition (Rapinel et al., 2019; Plakman et al., 2020), physiology (Wagner-Lücker et al., 2013) and structure (Straatsma and Baptist, 2008; Jalonen et al., 2015). Regionally, remote sensing has been successfully used to monitor similar grasslands (Thapa, 2011; Biswas, 2010; Acharya, 2002; Sarma et al., 2008), fires (Takahata et al., 2010; Ghimire et al., 2014) and channel migration of the Karnali River (Rakhal et al., 2021).

We aim to quantify spatio-temporal land cover change and establish relationships with the environmental drivers with focus on the ecologically important grasslands. We address both grasslands within the floodplain of the Geruwa River (the eastern branch of the Karnali River) and the grassland patches further away. Specifically, we give answers to the subquestions: (a) what is the spatio-temporal pattern of land cover; (b) what is the spatio-temporal variation in environmental drivers during the last three decades; and (c) what are the effects of environmental drivers on land cover change and what are possible mechanisms that explain these effects? We do so by mapping the historic development including recent annual dynamics of land cover with the use of field and remotely sensed data (LANDSAT). We then relate the land cover dynamics to abrupt changes in hydrological, meteorological and forest fire variables. The hypothesis is that between 1964 and 2019 a transition occurred from grasslands to later successional stages. The discharge distribution during peak discharges at the upstream bifurcation of the Karnali River would be a relevant driver for the vegetation pattern and associated habitats of megafauna.

2. Study area

2.1 Bardia National Park and Karnali River

Bardia National Park is located in the southwest of Nepal (Fig. 1) and was established as conservation area on 8 March 1976. The study area (135 km^2 of the now in total 968 km^2 of BNP) is delimited by (1) the Siwalik Hills in the north, where ephemeral streams originate that are tributaries to the Karnali River; (2) buffer zone and settlements in the southeast; and (3) the Geruwa Branch of the Karnali River in the west: a highly dynamic braided river system (Sinclair et al., 2017) located on the Karnali megafan (USAID, 2018). The Karnali River rises from Mt. Kailash on the Tibetan Plateau as one of the three biggest rivers draining Nepal. A few kilometres south of the Siwalik Hills near the town of Chisapani (Fig. 1) the Karnali River bifurcates into the Geruwa River (eastern branch) and Kauriala River (western branch), joining together in India as a tributary to the Ganges River. The subtropical climate in the region encompasses the monsoon, cool and dry post-monsoon, and a hot and dry pre-monsoon (USAID, 2018). Temperatures reach a maximum of 45°C in the hot season and fall to 10°C in January (Bolton, 1976). The mean annual precipitation is 1560 mm (DHM, 2017).
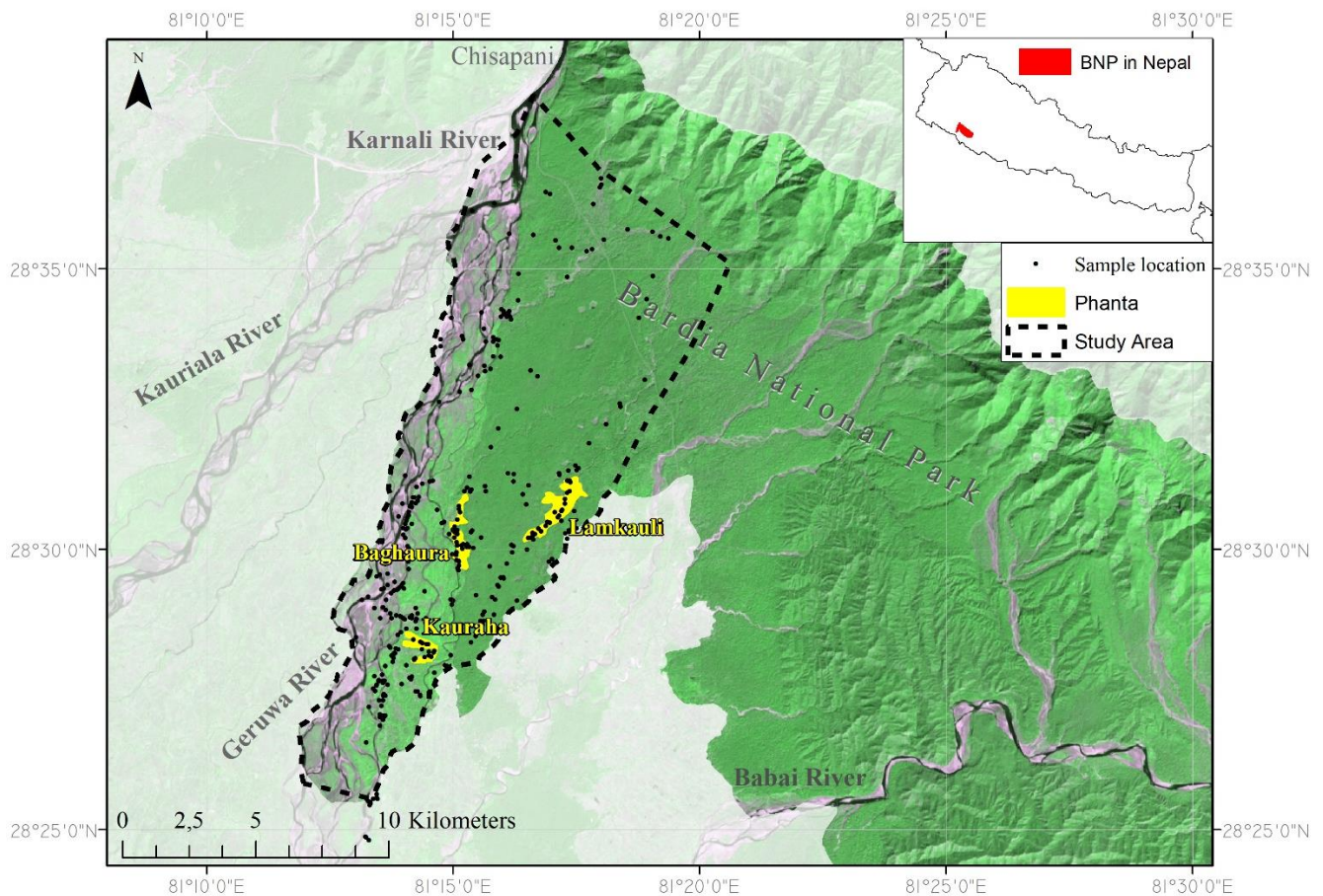
Figure 1: Delineation of Bardia National Park (dark green) and the study area (red) in and near the floodplain of the Karnali River. The megafan of the Karnali River lies between the two branches (the Kauriala and the Geruwa River) at the west side of Bardia National Park. This is a false colour composite (RGB = 656 of LANDSAT 8 imagery, 2020).

2.2 Drivers of grasslands in the Terai Arc Landscape and Bardia NP

135 Drivers in the form of physical disturbances vary in type, temporal components (frequency, duration, and timing), their spatial component (location, extent) and their intensity (White, 1985; Turner et al., 1998). In the TAL, both natural and anthropogenic disturbances are regarded as important drivers for grasslands in shaping the spatial and temporal patterns of vegetation. In BNP, fluvial process are regarded to be important at the landscape level. Flooding of the Karnali River and associated clearance of vegetation together with deposition of fresh alluvium have been observed (Seidensticker, 1976; Dinerstein, 1979a;

140 Lehmkuhl, 1989, 1994; Peet et al., 1999b). Fires occur in BNP on a yearly basis, and can be natural as well as anthropogenic. Forest fires occur most frequently in the Sal forest (*Shorea robusta* dominated) and in the months April and May (Ghimire et al., 2014). The phantas are annually set on fire by park staff (Dinerstein, 1979b; Peet, 1997). Appendix A provides an overview from the literature of the activities by locals and park staff (see also Thing et al., 2017 and Bhatta, 2000). After establishment as conservation area in 1976, free access for locals, who extensively relied on BNP for resources, was refused. Later on, active

145 habitat management was initiated on grasslands to compensate for the decreased disturbances. Permits that allow resource collection are needed for locals to enter the park for a certain number of days. Since 1983, the days of access and the number of permits issued increased until 1994 and 1999, respectively, and hereafter decreased drastically (Bolton, 1976; Bhatta, 2000). Whether the amount of permits in a given year and the days of access are proportional to the amount of removed biomass is not known (Bhatta, 2000). Before and around 1976, extensive grazing was recorded by cattle and wild ungulates in the south

150 west of the study area. The very short grazing lawns that are present in BNP are a result from patch-selective grazing by ungulates after cutting or burning (Thapa et al., 2021). Large herbivores can strongly influence the pattern and community structure of vegetation (Owen-Smith, 1988; Dinerstein, 1992). In the park, Asian elephant (*Elephas maximus*) (Ram and Acharya, 2020; Shrestha and Shrestha, 2021) and greater one-horned rhinoceros (rhino census in 2021) were virtually absent, but their numbers increased to 113 and 38 in 2021, respectively. Ungulates have been censused a number of times in BNP

155 (Dinerstein, 1980; Wegge and Storaas, 2009; Dhakal et al., 2014; Karki et al., 2016; Kral et al., 2017; DNPWC and DFSC, 2018, 2022). Some uncertainty is present around the numbers of ungulates, which have been debated in literature (van Lunenburg et al., 2017; Wegge et al., 2019). In BNP, the recorded densities of Chital deer (the most abundant mid-sized grazer) are: 53.99 (SE 10.29) (Dhakal et al., 2014), 29.3 (SE 4.3) (Karki et al., 2016), 56.44 (SE 5.75) (DNPWC and DFSC, 2018), 44.05 (SE 6.3) (DNPWC and DFSC, 2022).

160 **2.3 Vegetation types and successional stages**

Dinerstein (1979a) described six major vegetation types in the park, later modified into seven types (Jnawali and Wegge, 1993; Pokheral, 1993): alluvial tall grasslands (*Saccharum spontaneum* dominant), mixed tall grasslands (wooded grasslands), short grasslands (< 2 m, previously cultivated fields or 'phantas'), Khair-Sissoo forest, moist riverine forest, mixed hardwood forest and Sal forest. More detailed grassland associations are clarified in Appendix B (Lehmkuhl, 1989, 1994; Peet et al., 1999a;

165 Dinerstein, 1979a). The alluvial tall grasslands, which can be up to 4 m in height, consist of pioneer species that quickly cover bare alluvium after disturbance events. With no disturbances present, the line of succession is from alluvial tall grasslands via Khair-Sissoo forest to other riverine forest types, mixed hardwood forest or the climax Sal forest. Khair-sissoo forest is prevalent along the river courses and on floodplain islands in the Terai due to its ability to withstand floods. Sal forest consists of predominantly *Shorea robusta* trees that are fire resistant and is the most dominant tree species in BNP. Disturbances prevent

170 succession of alluvial grasslands to forest, turning them into mixed tall grasslands. If disturbances continue, short (< 2 m) and open grasslands may appear (locally called *phantas*) and their location is often more distal from stream channels (Dinerstein, 1979a; Lehmkuhl, 2000). A number of these grasslands are considered to owe their existence to human interferences such as

the Lamkauli, Bagaura and Khauraha phantas (Fig. 1) (Pokheral, 1993; Dinerstein, 1979b; Peet et al., 1999a). The largest phantas present are Lamkauli, Bagaura and Khauraha (Fig. 1). Nowadays, the phantas are predominantly vegetated with *Imperator cylindrica*, *Vitiveria zizanioides* and *Desmostachyia bipinnata* (Peet et al., 1999b). Within the mosaic of short and mixed tall grasslands, very short grazing lawns are present (Thapa et al., 2021). In the mixed tall grasslands (> 2 m) the *Narenga porphyrocoma* and *Erianthus ravennae* species are abundant and these grasslands are considered to lie on a continuum with the short grasslands (Peet et al., 1999b).

3. Data and Methods

3.1 Outline of approach

Figure 2 provides a flow chart of the methodology. We used topographic maps (1927, 1984) and aerial imagery of 1964 to assess the historic development of vegetation in the park and used LANDSAT imagery for reconstruction of annual land cover maps between 1993 and 2019. During the post-monsoon of 2019, BNP was visited to collect ground truth data of vegetation types. This dataset was used for supervised classification of land cover using a Random Forest model. From this time series, the areal extent, transitions and the pattern of land cover were calculated. These results were related to environmental variables (precipitation, discharge, fire occurrences) to provide insight in the dynamics of land cover and the response to variation in environmental variables.
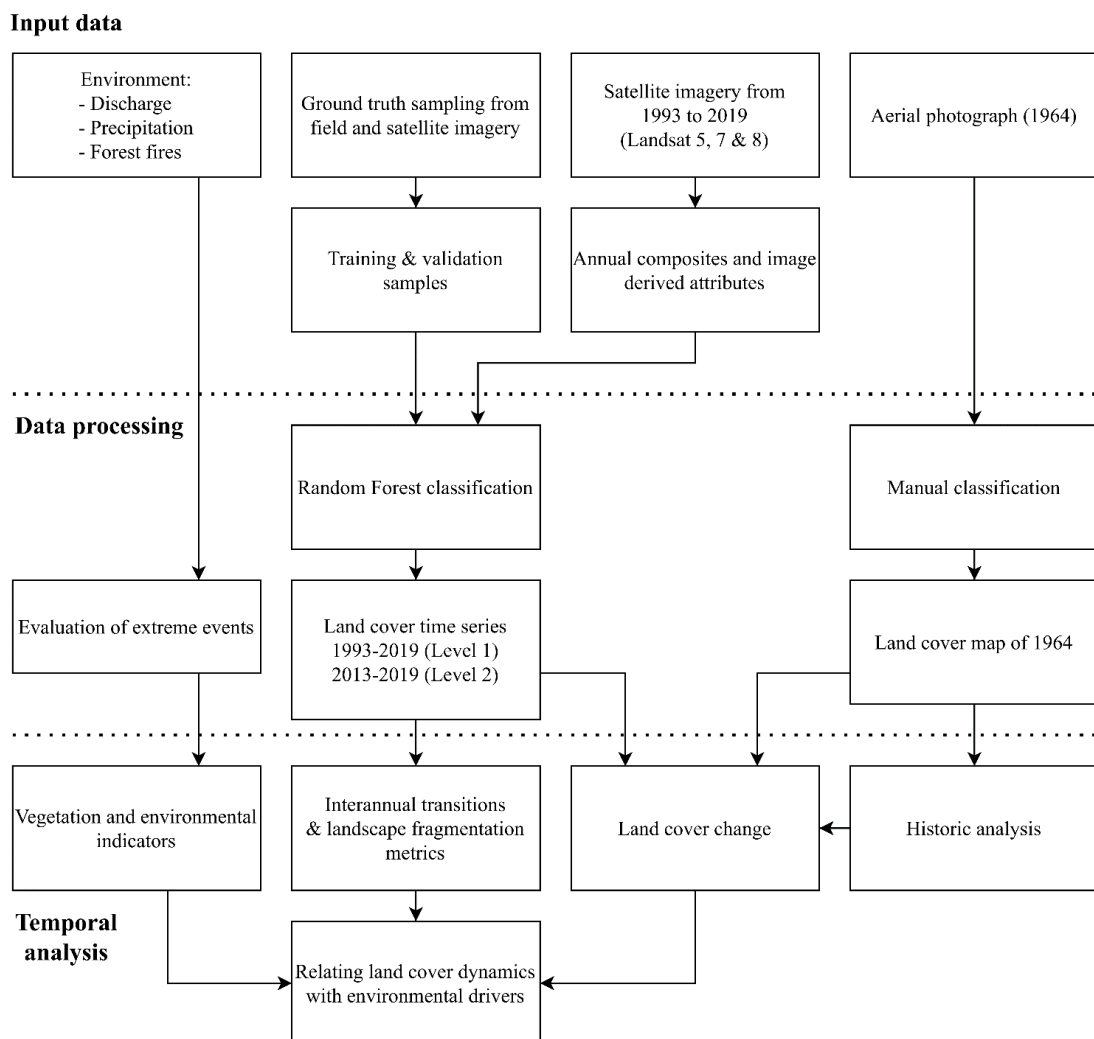
Figure 2: Flowchart showing steps from data sources to analysis.

3.2 Satellite imagery and aerial photographs

190 To establish a time series of yearly land cover, we selected imagery of the Surface Reflectance dataset (Tier 1) of LANDSAT 5, 7 and 8 satellites between 1993 and 2019. This imagery has a resolution of 30 m and the full pre-processing of the images is elaborated in Appendix B. The composites of 1995, 1997 and 2006 were not classified. Too few images of sufficient quality were available for 1995 and 1997 and a too large number of erroneous pixel values in the image composite was observed for 2006, caused by the LANDSAT 7 Scan-line error. For each year we calculated NDVI (Rouse et al., 1973; Rock et al., 1986;

195 Myneni et al., 1995; Beeri et al., 2007), NDDI (Gu et al., 2007), and Tasseled Cap Transformations (Crist and Cicone, 1984) and included seasonal information by forming seasonal composites and a harmonic trend analysis of NDVI. In addition, aerial photographs from 1964 were obtained from of the Forest Research and Training Centre, Ministry of Forests and Environment, Kathmandu. The individual photographs are combined and a point cloud is generated, followed by an orthomosaic with a resolution of 2-3 m (Fig. S1). The resulting orthomosaic with a resolution of 2-3 m was resampled to a resolution of 30 m to

200 compare it to the annual land cover time series.

3.3 Field data

Vegetation types were classified according to two schemes based on vegetation assemblages in Bardia NP (Appendix C) (Dinerstein, 1979b; Jnawali and Wegge, 1993; Peet et al., 1999a) and on remote sensing studies in similar environments (Biswas et al., 2014; Sarma et al., 2008; Thapa, 2011; Biswas, 2010; Arieira et al., 2011; Sharma, 1999; Dinerstein, 1979a).

205 The first land cover series (Level 1) contains four classes (water, bare substrate, grassland and forest) and spans from 1993 to 2019. The second series (Level 2) uses solely LANDSAT 8 imagery (2013 – 2019). The eight classes consist of water, bare substrate, alluvial tall grasslands, short grasslands, mixed tall grassland, shrubland, riverine forest and Sal forest (Appendix C). The height and cover of vegetation, together with the dominant species present were used to assign the vegetation types (Appendix D). These criteria enable discrimination between riverine grassland and non-riverine grasslands in the TAL (Biswas

210 et al., 2014). For short grasslands the height criterion of < 2 m is used. Shrublands (< 5 m) entail no distinct vegetation assemblage recorded in BNP, but was used in the TAL by Biswas (2010) and Sarma et al. (2008), and provided useful successional information on impact of disturbances in Canada (Hermosilla et al., 2018).

3.4 Classification & validation

The Random Forest model (Breiman, 2001) was used for classification, considering its earlier successful use in mapping of

215 vegetation in and near floodplains (Van Iersel et al., 2018; Belgiu and Drăgu, 2016; Harezlak et al., 2020). Two time series of land cover maps (Level 1 and Level 2) were created and the aerial photographs from 1964 was classified manually (Level 1) (Figure S1). For 2019, the classification model was trained on the image composites of 2019 with 70% of the field samples and the other 30% was used for validation. An error matrix was constructed for accuracy assessment and the user's and producer's accuracy was calculated (FAO, 2016). For classifying earlier years, all field samples were used to train a

220 classification model on the two seasonal image composites of 2019 and image derived attributes. The trained model for 2019 is transferable through time (Gómez et al., 2016). Pixels of each LANDSAT were then labelled with the most voted class for these pixels (Lawrence et al., 2006; Pal, 2005). To validate earlier years in the Level 1 time series, additional validation samples (106) were collected with publicly available imagery via Google Earth for the available years (2000, 2010, 2011 and 2018). The imagery was not detailed enough for delineation of the level 2 classes. A grid was created digitally with a distance of 1200

225 m between sample locations outside the floodplain and 600 m inside the floodplain.

3.5 Environmental drivers

3.5.1 Meteorologic and hydrologic data

Hydrologic and meteorologic datasets of the Karnali River were obtained from the Department of Hydrology and Meteorology office in Kathmandu. The datasets include the yearly maximum and minimum discharges, daily discharges and monthly
230 precipitation. This data was measured at the Chisapani weather station, north of the bifurcation and used to calculate hydrologic metrics (Table 1). Discharge has not been measured for the separate Karnali branches. Based on the dataset of 54 years of yearly peak discharges (Q_{peak}), extreme discharges (Q_{ext}) with $\geq$ 5-year recurrence times ($\geq 12,500$ m^3 s^{-1}) were identified using the Gumbel distribution (Gumbel, 1958). It has been postulated that discharges with these recurrences cause major changes in the river courses in the Ganga Plains (Thorne et al., 1993). The extreme precipitation events (P_{ext}) were identified by
235 considering the peak rainfall months for each year (P_{peak}). Thirdly, the switch of the dominant discharge branch of the Karnali River system at the megafan was identified (Sinclair et al., 2017; Dingle et al., 2020b). Fourthly, the position of the water-filled channels during the dry period was extracted from the annual land cover maps (Table 1). We performed change detection of these water-filled channels by considering the land cover maps of time steps *t* and *t + 1*, where *t* is 1 year. The results include newly covered area by water, disappeared water area and unchanged channels.

240 ### 3.5.2 Forest fires

A forest fire dataset from 2000 to 2019 was obtained from NASA's Fire Information for Resource Management System (FIRMS). The dataset contains detections of fire derived from sensors on satellites (MODIS and VIIRS). Pixels that detected fire are flagged and attributes such as the brightness, confidence of occurrence and time of day are added. The number of pixels that were flagged with presence of a fire were selected for each calendar year and we interpreted this number as the
245 area that burned. This enables identification of years with high forest fire activity. It should be reminded that this method results in an overestimation of the area that actually burned. The coarse resolutions (1 km for MODIS, 375 m for VIRS) limit information on the exact extent of the fire. When a fire occurs at the border of two pixels, the two separate pixels are flagged, doubling its detected area. Also, when two fires occur at the same time on a spatial scale that is smaller than the resolution of the imagery, they are flagged as a single detection. The metric of forest fires was expressed as the percentage of area that is
250 affected by fires for both the area within and outside the floodplain. For these two zones, the surface area is corrected for the areal extent of water and bare substrate.

Table 1: Datasets of the environmental drivers (A, B) and land cover dynamics (C), the derived metrics and their timespan.

A. Hydrological and meteorological data	Period	Derived metric
Discharge dataset: Yearly maximum and minimum discharge	1962-2015 1962-2015	Q_{peak} : Magnitude of yearly peak discharge (m^3 s^{-1}) Q_{ext} : Years where $Q_{peak} \geq 12,500$ m^3 s^{-1}
Precipitation dataset: sum of monthly precipitation (mm)	1964-2017 1964-2017	P_{peak} : Magnitude of the peak precipitation in a month for each year (mm) P_{ext} : Years with extreme precipitation events
Change in dominant discharge branch of the Karnali River	2009	Moment in time
B. Forest fires		
Number of pixels that detected fires	2000-2019 (MODIS) 2012-2019 (VIIRS)	Surface area yearly affected by detected fires, in- and outside of floodplain (%)

C. Land cover dynamics		
Land cover area of classes, Level 1 and Level 2 classifications	**Level 1:** 1993-2019 (excl. 1995, 1997, 2006) **Level 2:** 2013 - 2019	Yearly total area of each land cover class, within and outside floodplain (hectares)
Transitions of classes, Level 1 and Level 2 classifications	**Level 1:** 1993-2019 (excl. 1995, 1997, 2006) **Level 2:** 2013-2019	Interannual transitions of classes on pixel basis (hectares)
Channel dynamics: coverage of water class, based on Level 1 classification	**Level 1:** 1993-2019 (excl. 1995, 1997, 2006)	Yearly coverage of new, disappeared and unchanged channels in floodplain (hectares)
Pattern of grassland class	**Level 1:** 1993-2019 (excl. 1995, 1997, 2006)	PD, ED, AI and LSI (See Sect. 3.6 and Table 2)

3.6 Analysis of land cover dynamics

From the Level 1 time series, two metrics were derived representing land cover dynamics (Table 2). Firstly, interannual transitions between land cover classes were calculated on a pixel basis with yearly time steps (Mas and Vega, 2012). In total 16 combinations were calculated for the for the level 1 classification and 64 combinations for the level 2 classification. From these combinations we identified 'Removal of vegetation', which is the transition from forest and grassland towards bare substrate and water, and the 'Transition of grassland to bare substrate' (Table 2). Secondly, the land cover dynamics were characterized by their pattern with landscape fragmentation metrics. These metrics enable quantification of spatial patterns through time (McGarigal and Marks, 1995; McGarigal, 2002; Plexida et al., 2014) and have been used for similar ecosystems in the Terai (Biswas, 2010; Thapa, 2011). We then identified years where extremes in environmental drivers (Q_{ext} and P_{ext}) coincide with large interannual transitions of grassland to bare substrate (Table 2). This was substantiated with statistical tests (spearman tests in scatterplots) between the time series of annual extremes of environmental drivers (Q_{peak}, P_{peak}) and the interannual transitions of land cover (Tabel 2).

Table 2: The metrics that are used for establishing effects of drivers on land cover dynamics, including the method and the part of the study area that is considered. Lower half: fragmentation metrics used for quantification of the grassland pattern (McGarigal and Marks, 1995; McGarigal, 2002; Plexida et al., 2014). This part of the table is partly adapted from Sertel et al. (2018).

Land cover metrics	Description	Symbol	Method	Area
Removal of vegetation	Surface area (ha) changed of forest and grassland to the water and bare substrate.	Q_{peak}	Spearman	Floodplain
		Q_{peak}	Spearman	Floodplain
Transition of grassland to bare substrate	Surface area (ha) changed from grassland to bare substrate.	Q_{ext}	Coincidence	Floodplain
		P_{ext}	Coincidence	Outside FP
		Q_{peak}	Spearman	Floodplain
		P_{peak}	Spearman	Outside FP
Landscape fragmentation metrics				
Patch Density	Number of patches of corresponding patch type per unit area.	PD	Raster calculations	In- and outside FP
Edge Density	The sum of the lengths (m) of all edge segments in the landscape, divided by the total landscape area (m^2).	ED	Raster calculations	In- and outside FP
Landscape Shape Index	A standardized measure of patch compactness that adjusts for the size of the patch.	LSI	Raster calculations	In- and outside FP
Aggregation Index	A percentage that describes the ratio between the observed number of like adjacencies and the maximum possible number of like adjacencies, with respect to the proportion of the landscape compromised of each patch type.	AI	Raster calculations	In- and outside FP

4. Results

The spatio-temporal dynamics of the 27-years land cover series are first presented along with the historic analysis of land cover in 1927 and 1964 and 1984. Hereafter, the datasets on environmental drivers are presented and coupled to the yearly spatial extent of land cover classes and transitions from grassland to bare substrate.

4.1 Spatio-temporal land cover dynamics in BNP

4.1.1 Land cover maps

For the reference year 2019, the overall accuracies are 84.7% for the level 1 classification and 75.7% for the level 2 classification (Appendix E). The classes of mixed tall grassland and shrubland underperform for the level 2 classification. For the level 1 classification, the calculated accuracies were 75.5% (2000), 86.8% (2010), 84.9% (2011), 78.3% (2018) (Appendix E). Classes underperforming are bare substrate for the user's accuracy and water and grassland for the producer's accuracy.

A significant change in land cover (deforestation) around BNP can be seen when comparing the topographic maps of 1927 and 1984, particularly at the area in-between the Kauriala and Geruwa Rivers (SI I). A number of grassland patches observed between 1993 and 2019 can traced back to 1964 (Fig 3f). However, grasslands have shrunk in size and surrounding smaller patches completely disappeared (Fig 3f). The *phantas* Baghaura, Lamkauli and Khauraha are part of the remaining grasslands and consist of short and mixed tall grasslands (Fig 3). The Lamkauli grassland can also be observed on the topographic map of 1927 as the village, settlement or grassland of Lathwa. No signs of a village or agricultural fields are observed on the 1964 imagery, in line with the record that the Baghaura and Lamkauli phantas were cultivated after 1965 (Pokheral, 1993; Brown, 1995).

When traversing the study area from west to east, the classes encountered most abundantly are in turn: bare substrate, alluvial tall grasslands, short and mixed tall grasslands, shrubland, riverine forest and lastly Sal forest (Fig. 3d and 3e). Shrubland is located close to the perennial streams and the national highway that crosses the park from Chisapani to the eastern border of the study area. Sal forest forms a sharp boundary with other vegetation types coinciding with a difference in elevation that decreases southwards (Figure A2). Alluvial tall grasslands are dominant in and close to the active river channels and ephemeral streams, whereas shorter grasslands and mixed tall grasslands are located more distal from the active CHANNEL BELT (Fig. 3d and 3e). The active stream channels of the Geruwa River migrated westwards between 1964 and 2019 (Fig 3a and 3b). Also migration of individual channels is observed, for example the change of the dominant discharge branch in the northwest (Fig. 3b and 3c) and the abandonment a river channel southwest of the Baghaura phanta at 28.49 N°, 81.24 E°. This channel transitioned from an active river channel in 1964 (Fig. 3a) to grassland in 2000 (Fig. 3b) to forest in 2019 (Fig. 3c). Between 1993 and 2019, grasslands and low-flow river channels practically have covered the entire active CHANNEL BELT at least once, highlighting the dynamic nature of the braided river system (Fig. 3g). This indicates that the larger part of the riverine forest located in and close to the stream channels is not older than 27 years. Compared to alluvial tall grassland along the Geruwa River and ephemeral streams, the more distal short and mixed tall grasslands are present for a larger time span (Fig. 3h).
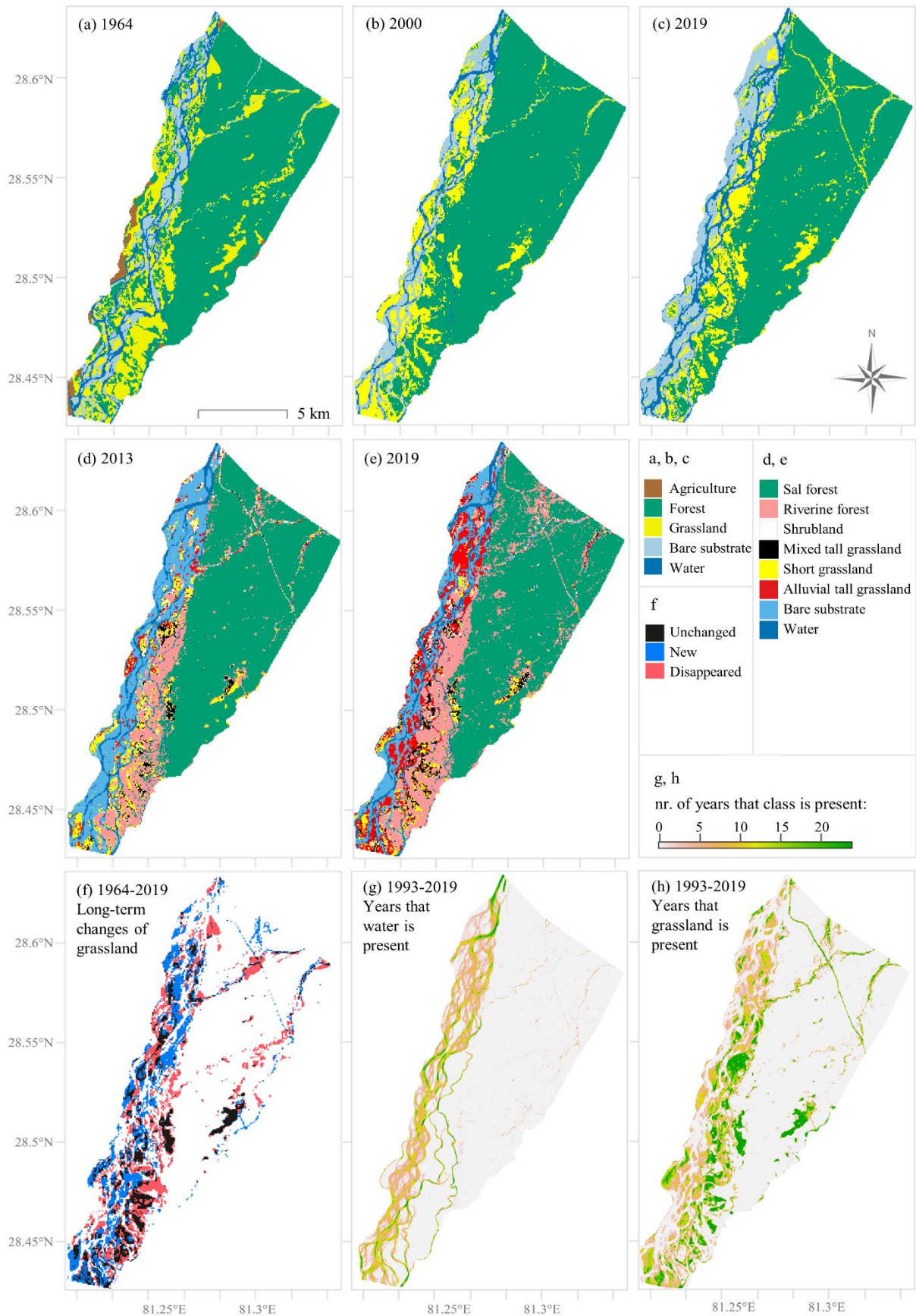
Figure 3: Overview of land cover maps. (a), the manual delineation of land cover classes from the aerial photograph composite of 1964; (b,c), level 1 data set; (d,e), level 2 data set; (f), the grasslands which are present in 1964 and during 2017-2019 and where they appeared and disappeared; (g,h), the number of years that water and grassland in total was present during the time period 1993-2019 (calculated from level 1 data set). The full series of land cover maps is presented in Figure A3 .
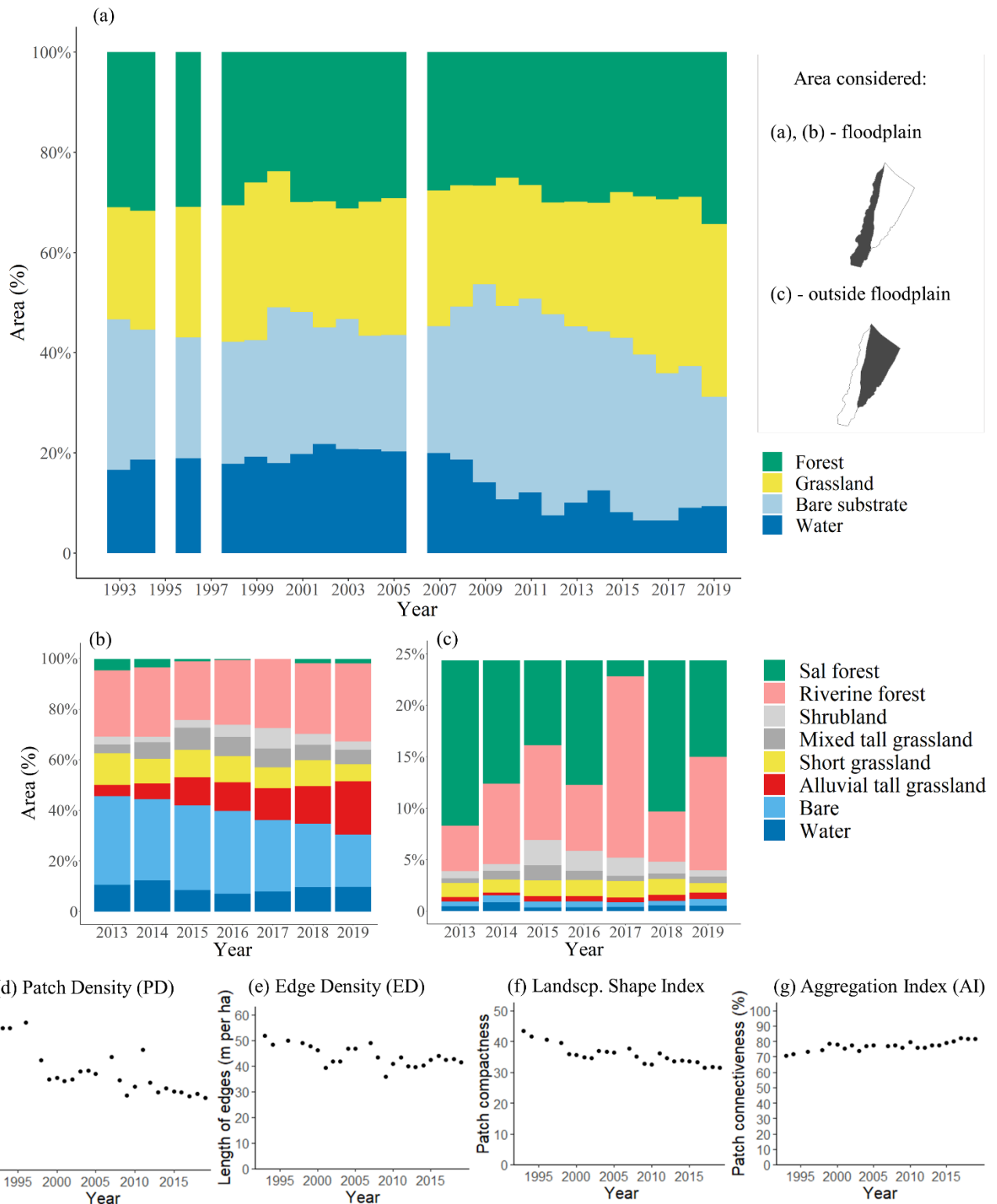
Figure 4: The temporal changes in land cover classes and pattern. (a), level 1 dataset; (b,c), level 2 dataset. White columns represent years with no data. Water can be interpreted as average water cover during the dry season. Note that a maximum of 25% was set in (c) for the surface area outside the floodplain for visualisation purposes; the remaining 75% of the area consists solely of Sal forest; (d,e,f,g), landscape fragmentation metrics (Table 2) through time for the grassland class in the floodplain, derived from the level 1 dataset .

4.1.2 Land cover dynamics 1993 – 2019

Within the floodplain, succession and retrogression are observed in the Level 1 classification (Fig. 4a) from which three periods can be distinguished: 1993-1999, 2001-2008 and 2010-2019. These periods are characterised by a gradual decline in the areal extent of bare substrate and an increase of vegetation, particularly grassland. The three periods are separated by years wherein the surface area of bare substrate increased considerably as compared to the year before (2000; 2008 and 2009). In the first period, grassland is in an increasing trend until 1998. In this period, water covers on average 18% of the floodplain, amounting to 932 ha. In the second period (2001-2008), the area covered by water (low flow channels) was slightly larger (1020 ha on average), while forest gradually decreased and grasslands saw an increase. In the third period (2010-2019), the area of bare substrate and water decreased to the lowest value since 1993. Bare substrate decreased gradually, whereas the coverage of water halved more abruptly to 478 ha on average (-53%) as compared to the second period (2001-2008). The level 2 classification confirms the expansion of vegetation (Fig. 4b). This expansion most evident in the floodplain where the surface area of alluvial tall grassland increased from 280 to 1185 ha. The short grasses and mixed tall grasslands do not show such a trend. A notable decline of forest is observed in 2015, both on the floodplain (Fig 4b, to grassland) and outside of the floodplain (Fig. 4c). The grassland pattern shows a decrease of heterogeneity in the landscape: the number of patches decreased (Patch Density, Fig. 4d), the length of the edges of grassland with other classes decreased (Edge Density, Fig. 4e), the patches have become more compact (Landscape Shape Index, Fig. 4f) and the patches have become more connected to each other (Aggregation Index, Fig. 4g).

4.2. Environmental drivers

The discharge regime of the Karnali near Chisapani is characterised from 1993 to 2015 by a large seasonal variation, with a mean discharge of 1,389 m^3/s, a minimum of 173 m^3/s and a maximum of 21,700 m^3/s in August 2014. The median is 678 m^3/s. Extreme discharges of the Karnali River can be up to three times the yearly average peak discharge. The monthly precipitation dataset shows a similar monsoonal variation, with a mean monthly rainfall of 196 mm and a maximum of 1,673 mm, a minimum of 0 mm and a median of 40 mm. For the studied period of 1993-2019, Fig. 5a shows the extreme peak discharges (Q_{ext}) with a recurrence time of more than 5 years as calculated with the Gumbel distribution and it also displays the periods with extreme precipitation (Pext in Fig. 5b). An overview of the daily discharge measurements is shown in Figure A4. The peak discharges of the daily and yearly dataset do not have the exact same values, but are in statistical correspondence to each other. We based our analysis on the yearly discharge dataset. Two months with extreme conditions were identified in 2007 and 2014, of which the second largest with 1560 mm for the monthly maximum (in 2007) is 47% larger than the third largest event (Fig. 5b). On an annual basis, the highest cumulative precipitation was recorded for the same years: in 2007 and 2014 with 3,293 and 3,390 mm, respectively.

Forest fires were most abundant in the study area in the years 2012, 2013, 2014, 2016 and 2019, based on both the MODIS and VIIRS detection datasets (Fig. 5c and 5d). As of 2012 and onwards, the variance of the yearly affected area by fires in the floodplain increased: the maximum surface area affected increased, alternated with years wherein the surface area affected was very low. The channel dynamics were quantified by comparing the annual location of the stream channels in the dry period. The newly covered surface area of channels has decreased considerably after 2009 compared to the years before 2009 (Fig. 5e). Most changes in surface area took place in the years 2007, 2008 and 2009, whereafter the average absolute area that changed decreased.
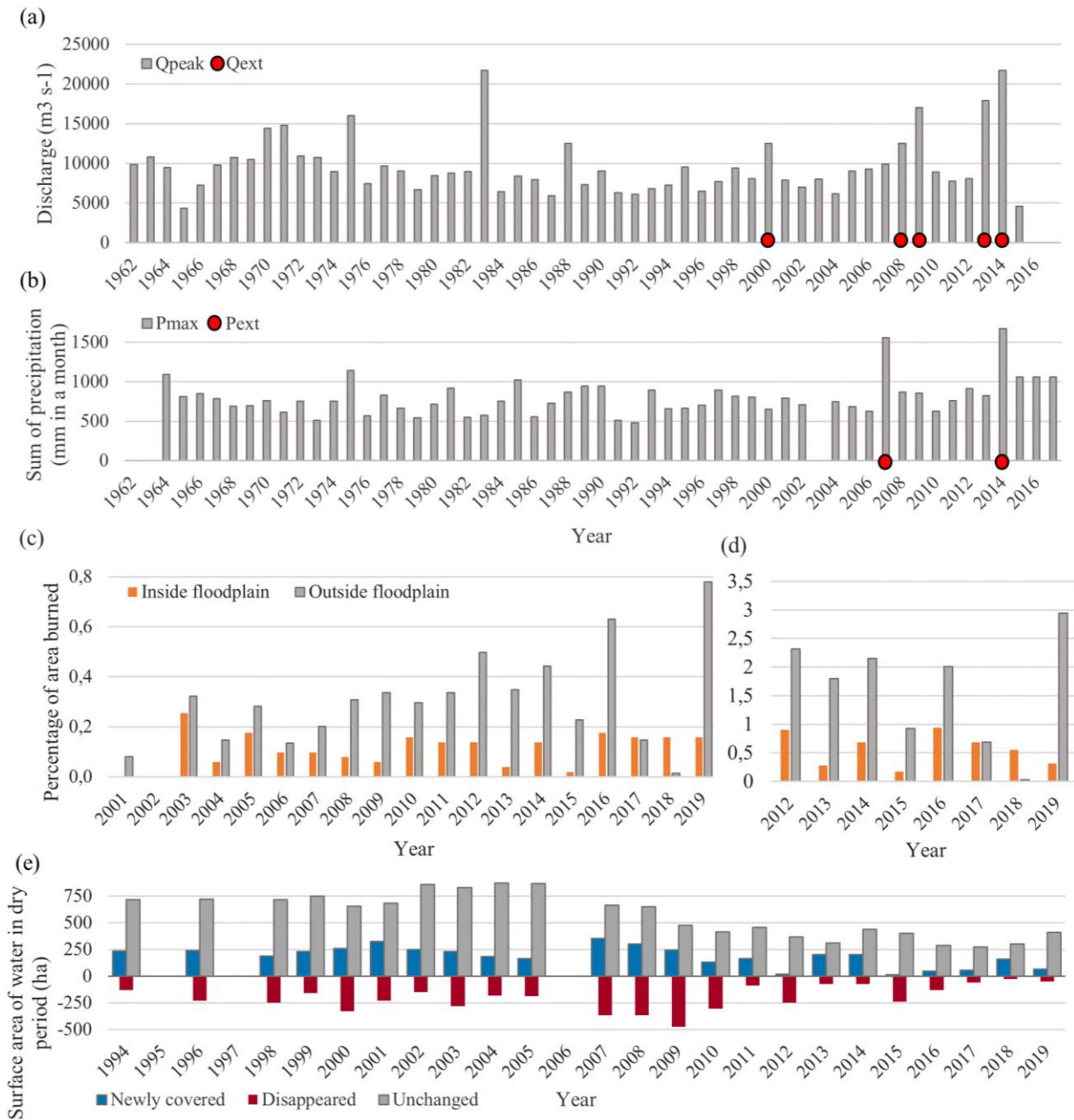
Figure 5: Environmental drivers. (a) Yearly maximum peak discharge (Q_{peak}) and identified extremes (Q_{ext}) are shown for the discharge dataset; (b) For each year the month with the most precipitation (P_{max}) is shown, along with the identified extreme years (P_{ext}); (c,d), surface area affected by fires in and outside the floodplain as detected from the MODIS (c) and VIIRS (d) datasets, respectively; (e) Change in surface area (hectares) covered by channels for each year compared to previous year; newly covered, area covered by new channels; disappeared, area abandoned by channels; unchanged, area covered by channels in current and previous year.

4.3. Relating environmental drivers to land cover dynamics

For the years 2000, 2008 and 2009, when extreme peak discharges occurred, a response in vegetation is observed in the floodplain in the form of increased transitions from grassland to bare substrate (Fig. 6a). These increased transitions are not observed for 2013 and 2014, while in these years the recorded peak discharges were higher than in 2000, 2008 and 2009. The

major change of the river course occurred in 2009, when the dominant discharge branch relocated from the Geruwa River (in our study area) to the Kauriala River. The extreme discharges in 2009 most likely have markedly changed the channel geometry, with a decrease in retrogression events after its relocation. This is also supported by the results of areal development of land cover (Fig. 4), where, before the channel relocation, the area of bare substrate only increases in the years that experienced extreme discharges, and surprisingly not after the channel relocation in 2013 and 2014. Outside the floodplain (Fig. 6b), close to ephemeral streams the large transitions of grassland to bare in 2007 and 2014 coincide with years that experienced extreme precipitation events. These transitions occurred mostly near the ephemeral streams, on a much smaller (20 times) as compared to the floodplain of the Karnali River.

For yearly peak discharges, a significant ($p < 0.05$) positive correlation is present between the maximum discharge in a year and the areal change from grassland to bare substrate within the floodplain in the period between 1993-2009 (Fig. 6c). This is not the case for 2010-2019 ($p > 0.05$), where the high peak discharges of 2013 and 2014 experience no increased transitions from grassland to bare compared to years with average peak discharges (Fig. 6d). Outside of the floodplain, extreme rainfall events and grassland to bare transitions show no correlation ($p > 0.05$), but the extreme precipitation months of 2007 and 2014 coincide with the highest transitions from grassland to bare (labelled in Fig. 6e).
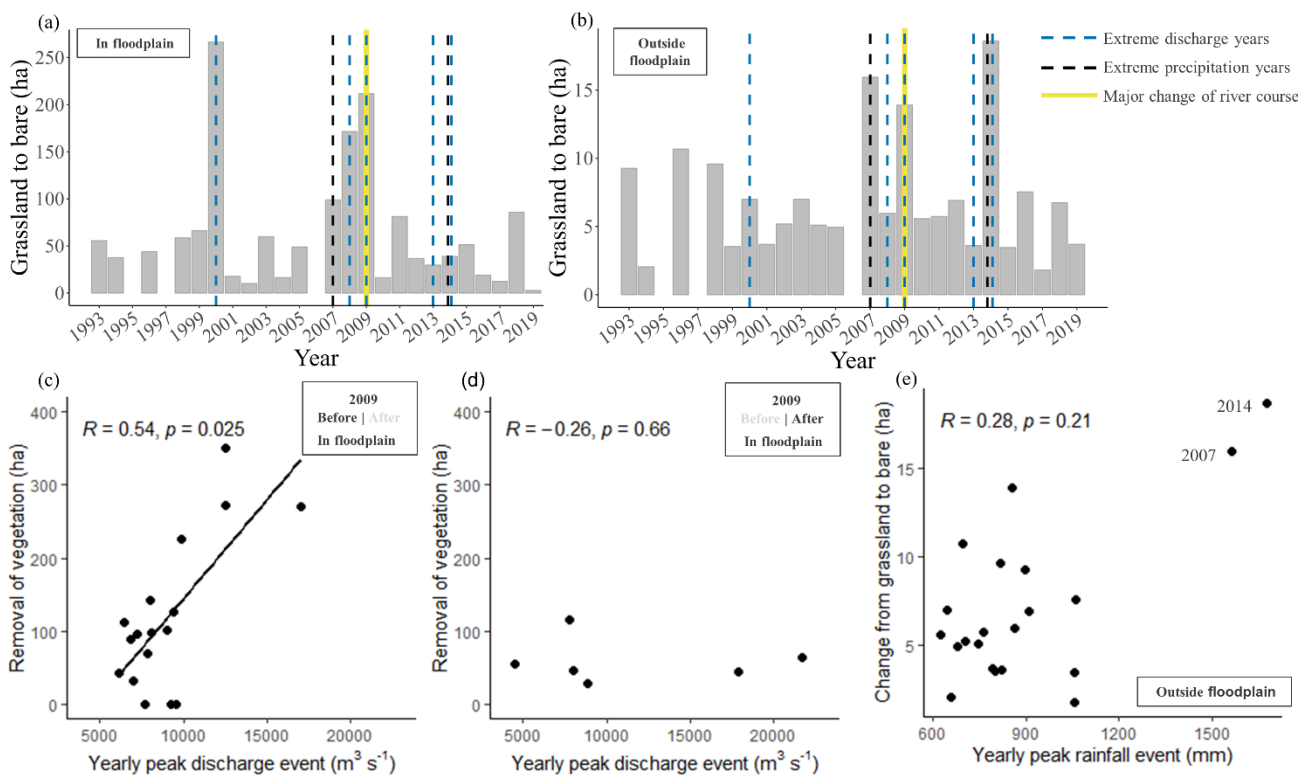
Figure 6: Environmental variables related to land cover dynamics derived from the Level 1 classification series. (a, b), annual transitions from grassland to bare substrate in hectares (orange bars), years that experienced extreme discharge events (> 12,500 m³/s) and peak precipitation events within the floodplain (a) and outside the floodplain (b). Panels (c), (d) and (e) show correlation tests of environmental and land cover variables. (c) and (d) show the annual removal of vegetation (the transition of Sal forest and grassland towards water and bare substrate) as related to the magnitude of yearly peak discharge before the channel relocation (c) and after the channel relocation (d); (e) shows the yearly peak rainfall events (mm in a month) and the transition of grassland to bare substrate. Note the difference in scale on the y-axes.

5. Discussion

We analysed the spatio-temporal dynamics of land cover in Bardia National Park and the effects of environmental drivers and variation therein on these dynamics. The results are discussed and compared to similar ecosystems at the foot of mountain ranges. As land cover acts as a biophysical indicator of the state of an ecosystem (Meyer and Turner, 1992; Henderson-Sellers and Pitman, 1992; Hansen and Loveland, 2012), the implications for BNP and possible cascading consequences for the ecosystem and nature management are also considered.

5.1 Evaluation of obtained accuracies and limitations

The observed temporal trends in land cover echo natural trajectories of succession, apart from the rapid forest recovery observed in the years 1999-2000 and the unrealistic fluctuations in riverine and Sal forest for the level 2 classification. The accuracies are similar to contemporary studies (Hermosilla et al., 2018; Harezlak et al., 2020; Van Iersel, 2020). Therefore, we argue that the series of land cover maps are of sufficient accuracy (76%-87% for Level 1, 75% for Level 2) to draw conclusions on the general trends in land cover dynamics in the Geruwa River floodplain and adjacent part of Bardia National Park. The decreased surface area of grasslands is in accordance with observations in previous studies (Peet et al., 1999b; Jnawali and Wegge, 2000; Odden and Wegge, 2005; Neupane et al., 2020). Between 1976 and 1997, Odden (2007) recorded a decrease of grassland (-8%) in the southwest of the study area. Between 1990 and 2013, Neupane et al. (2020) recorded a decrease in the surface area of grasslands from 31% of the total surface area in BNP to 17% (-45%). In this study we recorded a decrease of -35% between 1964 and 1996. The differences in numbers could be due to: (1) the studies differ in time span studied; (2) the studies differ in area studied; (3) the studied years are in another phase of the biogeomorphologic cycle (Corenblit et al., 2007), causing the areal extent of floodplain grasslands to differ greatly prior to or after a flood. This cycle is also reflected in our results (Fig. 4); (4) the methods to construct land cover maps differ. Uncertainties in our results could originate from the classification models used, the input data (field samples and satellite image composites), validation data (collected in the field and with Google Earth), the change detection algorithm, and the datasets of the environmental drivers.

5.2 Land cover dynamics from 1964 to 2019

The deforestation outside BNP is in line with the general observation that the TAL experienced high rates of deforestation in the previous century, but in contrast with the encroachment of forest within BNP in the past decades. The total areal extent of grassland was higher in 1964 (2614 ha) than in 2019 (2114 ha). Our interpretation is that short grasslands were proportionally more abundant in 1964 than in 2019 and vice versa for the alluvial tall grasslands, which expanded to 1184 ha in 2019 (Dinerstein, 1979b). Dinerstein (1979b) recorded that vegetation west and southwest of the Baghaura phanta was grassland with dispersed trees in 1976, which is in line with our findings for 1964. In 2019, this location is almost entirely covered by riverine forest (Fig. 3a and Fig. 3e). This is also the case for the Mansuri phanta, north of the Lamkauli phanta, which was a grassland up to 1976 but has converted to forest due to succession (Fig. 3f) (Bhatta, 2000).

The period between 1993 and 2019 shows gradual successional changes and years with abrupt retrogression events. A decrease of heterogeneity of the grassland pattern is observed from 1993 to 2019, because grassland patches decreased in size and abundance and became more rounded and compacted. Riverine forest is observed in both the Karnali floodplain as well as along ephemeral streams. Bolton (1976) recorded the latter as an *'undescribed riverine forest type'*. Bare substrate is quickly colonized by early successional tall grassland. Concurrently, a portion of these grasslands transition towards the later successional grasslands and forests, but at a slower rate. Lehmkuhl (1989) pointed out these different rates of succession for

vegetation in Chitwan National Park. It is of interest to which extent the alluvial grasslands and riverine forest eventually expand, as in the last decade their combined area shows an increasing trend.

5.3 Environmental drivers

5.3.1 Hydrologic and meteorological drivers

440 The large discharge and precipitation fluctuations are associated with the monsoonal climate at the foot of mountain ranges (USAID, 2018) and alluvial megafans (Leier et al., 2005) such as the Karnali megafan.and Kosi megafan. In 2014, the extreme precipitation in BNP and extreme discharge of the Karnali River coincided. Extensive loss of landmass and destruction of houses was recorded (Sinclair et al., 2017), and extreme flooding was also recorded in the nearby Babai River in BNP (Chhetri et al., 2020). During the peak discharge in 1983, in magnitude second to the discharge in 2014, extreme flooding (MacClune

445 et al., 2014) resulted in coverage of the Baghaura phanta with sediment (Bhatta, 2000). Between 1993 and 2019, we observed no conversion from grassland to bare substrate on this phanta. The active stream channels of the Geruwa River migrated westwards, which was also recorded by Rahhal et al. (2021).

For 2009 there are indications that a major redistribution of discharge occurred at the apex of the Karnali megafan. Dingle et

450 al. (2020) suggested, based on LANDSAT imagery, that the western branch was already dominant in 2001. This is not reflected in the results of the annual land cover time series of this study, which show a relocation of the main discharge in 2009. In addition, the rate of channel migration declined since 2009 and the water coverage in the Geruwa River decreased in the dry period (-53%). In contrast, Rakhal et al. (2021) found an increase in long term channel migration in the eastern branch of the Karnali River between 1977 and 2013. The cause for the discrepancy can possibly be found in the time span studied: the last

455 decade (2010-2019) was not fully assessed by Rakhal et al. (2021) and the large-scale channel migrations in 2008 and 2009 could dominate the signal. During low discharges, the current distribution of discharge is considered to be about 80% for the Kauriala River and 20% for the Geruwa River (Sinclair et al., 2017; Dingle et al., 2020a). During peak flow of monsoonal discharges, the distribution is thought to be higher in the Kauriala River (55-65%) (Dingle et al., 2017, 2020a). Time scales associated with avulsions at the apex of the Karnali megafan are estimated to be between ~400 and 7,000 years, (Dingle et al.,

460 2020b), suggesting that the new discharge situation at the apex could hold for centuries. It is estimated that a discharge of 23,500 m^3 s^{-1} to 31,500 m^3 s^{-1} is required to entrain the coarse gravel near the apex of the Karnali megafan (Dingle et al., 2020b). This is higher than the discharge measured in 2009 (17,000 m^3 s^{-1}) that caused the channel relocation. Altogether, indications are very strong that indeed a major change in channel geometry occurred and consequently a redistribution of discharge, resulting in more static hydromorphological processes in the Geruwa River. If erosion and sedimentation rates

465 decrease, also rejuvenation of the floodplain decreases (Gunderson, 2002; Corenblit et al., 2007). The extreme peak discharges are not the sole hydrological driver for vegetation (Pickett et al., 1987; Corenblit et al., 2007). For example, prolonged inundation is common in a number of conservation areas in the TAL that are more characterized as wetland complexes, such as in Chitwan National Park (Dinerstein, 1979a). Our interpretation is that that prolonged inundation is less of an important driver in BNP than in Chitwan National Park.

470 ### 5.3.2 Forest fires, anthropogenic disturbances and herbivory.

The variance of area affected by forest fires between years increased: the surface area affected (predominantly outside the floodplain) was large in the years 2012, 2013, 2014, 2016 and 2019, with increasing maxima. Ghimire et al. (2014) found that the surface area that burned increased after 2008, and increase that we recorded since 2012. Ghimire et al. (2014) suggested

changing climatic conditions as an explanation. We interpret the anthropogenic disturbances in relative terms, based on the days of access for locals, the yearly amount of permits issued for resource collection and what is known from literature on management activities (Appendix A) (Bolton, 1976; Brown, 1998; Bhatta, 2000; Bhattarai et al., 2017; Thapa et al., 2021). Anthropogenic disturbances by locals have strongly diminished since the establishment as a protected area in 1976, thereafter increasing towards the passing of the millennium, again followed by a considerable decrease (Bolton, 1976; Dinerstein, 1979b; Brown, 1995; Bhatta, 2000; Thapa et al., 2021). Persistent presence of (grazed) short grasslands is still observed on the channel bars southwest as confirmed by field observations on that location (Fig. A5). Maintenance by park staff also seem to have increased towards the passing of the millennium (Bhatta, 2000) and was extensive in recent years.

Herbivory effects land cover in a more gradual way than the pulse disturbances considered in this study, and therefore we do not attribute this driver to the abrupt vegetational changes. On the long term, interpretation of grazing pressure on the vegetation pattern is hindered by uncertainty around the development of numbers of livestock and wild herbivores before and after the establishment as conservation area. In 1975, biomass of livestock was 15-17 times higher 47,959 kg km^{-2} than biomass of wild ungulates in 1977 (2842–3120 kg km^{-2}) in the southwestern part of the study area (Dinerstein, 1980). Between 1976 and 1999, grazing by livestock decreased and ungulates are thought to have increased fourfold in numbers (Wegge and Storaas, 2009). It is of interest whether wild herbivores could have compensated for the decline in grazing pressure by livestock, on which no consensus exists in literature (Karki et al., 2016; van Lunenburg et al., 2017; Wegge et al., 2019).

5.4 The effects of drivers on land cover dynamics

For the period before 2009, the results show a correlation between the transitions of grassland to bare substrate and the magnitude of yearly peak discharge. This relation is absent after 2009, although in 2013 and 2014 the peak discharges were of a higher magnitude than in 2009. This indicates that the impact of hydromorphological disturbances on vegetation in the floodplains of the Geruwa River decreased considerably during extreme discharges of the Karnali River. The absence of retrogression events during extreme discharges of the Karnali River in 2013 and 2014 contrasts with our hypothesis that in Bardia National Park extreme discharges of the Karnali River always cause a removal of vegetation, followed by a period of regrowth. The reduced hydromorphological dynamics favour transition to later successional stages of vegetation in the floodplain (Corenblit et al., 2007). This is in accordance with our observed expansions of alluvial tall grasslands and to a lesser extent that of riverine forest after 2009. The two most extreme precipitation events coincide with the largest transitions from grassland to bare substrate in the area outside of the floodplain along the ephemeral streams. Only during extreme precipitation events the magnitude of erosion and sedimentation processes seem large enough to convert vegetation to bare land, because no correlation was found between the yearly maxima of precipitation and the retrogression of grassland. On the spatial and temporal scale of this study, no signal was detected between the transitions of land cover classes and years with extensive forest fires. We interpret the forest fires not to be a principle factor that converts forest towards grassland, which was also suggested by (Lehmkuhl, 2000). However, fires do play an important role in maintaining grassland (Peet et al., 1999b; Bhatta, 2000; Lehmkuhl, 2000).

Altogether, we attribute the decrease in surface area and abundance of grassland patches to, firstly, the reduced anthropogenic disturbances by locals since the establishment as protected area in 1976. Secondly, the westward migration of channels in the Geruwa River is followed by succession to later successional stages in the abandoned channels of the Geruwa River. The contrasting recent expansion of alluvial tall grasslands is attributed to a decline in hydromorphological dynamics in the Geruwa floodplain. Phantas such as Lamkauli, Baghaura and Khauraha experienced significantly less encroachment than surrounding

smaller patches. This is attributed to anthropogenic maintenance practices that are predominantly executed on these phantas, in contrast with the surrounding smaller grassland patches. If the grasslands would have been left unmanaged, encroachment of the forest would have been more severe.

5.5 Global comparison

Disturbance-dependent grasslands, especially those located in high rainfall regions, are threatened by indigenous forest expansion, which has been recorded in Australia, Africa, India and North and South America (Puyravaud et al., 2003; Banfai and Bowman, 2006; Silva et al., 2008; Wigley et al., 2009). Grasslands in the Nepalese TAL can be added to this list. The redistribution of discharge through the two branches is thought to have had a profound impact on land cover. A comparison is made to parable conservation areas near lowland alluvial megafans. In the Pantanal (Brazil), extreme hydrologic conditions are explicitly analysed as a driving force in the pattern of vegetation communities (Arieira et al., 2011). The Taquari megafan in the Pantanal experienced a shift in environmental drivers due to an avulsion, increasing susceptibility to deforestation and fire (Louzada et al., 2020). At the foot of the Himalayas in northeastern India, extensive vegetational changes towards dryer vegetation types occurred after shifts in river courses in Jaldapara Wildlife Sanctuary (Biswas et al., 2014) and in Manas National Park (Sarma et al., 2008). In Jaldapara Wildlife Sanctuary, floods in 1968 caused a relocation of the Torsa River. This is regarded as one of the primary drivers that caused a transition of grassland towards woodland (Biswas et al., 2014). For the Manas National Park, Sarma et al. (2008) stated that after the relocation of the river, the change of grassland to forest could have been partly prevented by more active management of the grasslands

These analogous scenarios demonstrate the possible consequences for BNP, namely a change in the (relative) dominance of environmental drivers, and possibly a shift towards dryer vegetation types and an increased susceptibility to droughts and fires. Without increased disturbances from another driver, for example anthropogenic disturbances, one could expect that a proportion of the now extensive alluvial tall grassland transition to a more homogenic (riverine) forest, especially considering the decreasing trend of heterogeneity of grassland in the landscape. This evokes questions on the degree that humans should intervene in a (semi-)natural system. The importance of 'human-dependent' habitat is also interesting in the light of how grasslands are described in literature. Classically, grasslands are seen as a transitional land cover from a successional point of view (Clements, 1916), while recent studies highlight the importance to subdivide grasslands from a conservation perspective (Buisson et al., 2019; Bond and Parr, 2010) into old-growth (or ancient) grasslands (Bond, 2008; Veldman et al., 2015) and cultural (or derived) grasslands. The old-growth grasslands are regarded to harbour a higher biodiversity and endemism when compared to the cultural grasslands. In contrast to this subdivision for conservation goals, subtropical grasslands in the TAL that are remnant of anthropogenic occupation and cultivation (the phantas) serve an important ecosystem role for tiger conservation goals in Bardia National Park by sustaining prey populations.

5.6 In perspective of megafauna

Migrating channels at the apex of the Karnali megafan and associated redistribution of discharge are connected to the land cover distribution in the western part of BNP, and with it, habitat of threatened megafaunal species. With the recent ongoing increase of grassland near the Geruwa River, the spatial extent of favourable habitat for species that depend on alluvial tall grasslands, such as greater one-horned rhinoceros and hog deer (Jnawali and Wegge, 2000; Odden et al., 2005; Pradhan et al., 2008), increased, but the natural mechanism that maintains these early successional tall grasses has reduced in strength. In Chitwan, habitat heterogeneity was positively correlated with the abundance and habitat preference of prey species of tigers (Bhattarai and Kindlmann, 2012). Moe and Wegge (1994) suggested that a high density of ungulates in BNP is possible due

to the fine mosaic pattern of habitats in the Karnali floodplain. However, heterogeneity of grasslands in BNP shows a decreasing trend. This could be unfavourable for Chital deer and tiger, although their numbers suggest otherwise. Tiger population showed the largest increase in BNP among the conservation areas in Nepal (DNPWC and DFSC, 2022), particularly due to conservational efforts.

5.7 Future Research

In the next decades, changes in the environmental drivers are projected because of, amongst others, changing climatic conditions. Precipitation, temperature and mean annual discharge are projected to increase in the Karnali River basin except for the post-monsoon, when smaller amounts of precipitation and discharge could be expected (Dahal et al., 2020; Rakhal et al., 2021). The combination of earth observation with time series of environmental drivers adds to the understanding of spatio-temporal dynamics of land cover and proves to be useful for monitoring with minimal monetary costs. With future technological advances in mind, the algorithm could be improved upon (e.g. Hermosilla et al., 2018; Van Iersel, 2020) to enable detailed analysis of vegetation dynamics on the community or species level, including invasive species (Bhatta et al., 2020). In addition, further research on the drivers and the changing relative dominance will aid conservational effort and management decisions in BNP and similar nature reserves where disturbance-dependent grasslands are under threat of forest intrusion.

6. Conclusion

We aimed to quantify the spatio-temporal land cover change and establish relationships with the environmental drivers. This was done in Bardia National Park (BNP), located along the highly dynamic Karnali River at the foot of the Himalayas in a climate conductive of forest growth. We focussed on disturbance-dependent grasslands that are vulnerable to encroachment. Grasslands in the floodplain of the Geruwa branch of the Karnali River and the adjacent part of BNP were more abundant and were located more eastwards in 1964 than between 1993 and 2019. Between 1993 and 2019, grasslands showed a steady decline in heterogeneity, pinpointing the decrease in size and abundance of the patches. The more recent ongoing increase of surface area of grasslands can be attributed to expansion of alluvial tall grasslands in the floodplain. The maximum surface area affected by forest fires increased, but at the same time affected surface area became more variable between years. Since 2009, the Geruwa branch of the Karnali River was partially abandoned. Before 2009, the magnitude of discharge events shows a correlation with transitions from grassland to bare substrate. This correlation is not present anymore after 2009 and no increased transitions are observed for 2013 and 2014, while the recorded peak discharges were of a higher magnitude in these years. Also, the channel dynamics of the eastern branch of the Karnali River decreased since 2009. Hence, we confirm our hypothesis that from 1964 to 2019 a shift occurred from grasslands to riverine and Sal forest. This shift is predominantly attributed to a westward shift of the active stream channels of the Geruwa River and the establishment as conservation area in 1976 with associated reduced anthropogenic disturbances by locals. The more recent expansion of alluvial tall grasslands is attributed to the redistribution of discharge in 2009 of the Karnali River. In 2019, land cover in the floodplain is more favourable for faunal species that depend on alluvial tall grasslands such as hog deer (*Hyelaphus porcinus*) and greater one-horned rhinoceros (*Rhinoceros unicornis*), although the mechanism to maintain these grasslands reduced in strength. For faunal species that benefit from a heterogenic vegetation pattern, land cover is thought to have become less favourable between 1964 and 2019 as the heterogeneity and surface area of the grassland patches decreased. Because hydromorphological processes in the floodplain have become more static, other agents of disturbances are more paramount to prevent encroachment of grasslands.

Data availability

Data is available via the contact person by sending an email to jitsebijl@xs4all.nl.

Acknowledgments

595 The authors are grateful to officers of the government of Nepal and in particular Dipesh Kumar Sharma, Assistant Research Officer at the Forest Research and Training Centre, Ministry of Forests and Environment, Nepal, for helping with the acquirement of the aerial imagery and topographic maps. We thank the people from NTNC for their great help and support during field work. We acknowledge the use of data from NASA's Fire Information for Resource Management System (FIRMS) (https://earthdata.nasa.gov/firms), part of NASA's Earth Observing System Data and Information System (EOSDIS). We thank reviewers for valuable comments on a preprint of the manuscript

600 Competing interests

The authors declare that they have no conflict of interest that could influence the work reported in this paper.

References

Acharya, R.: Comparison of change detection techniques in Chitwan District of Nepal, Change, 1–12, 2002.

Alaibakhsh, M., Emelyanova, I., Barron, O., Sims, N., Khiadani, M., and Mohyeddin, A.: Delineation of riparian vegetation
605 from Landsat multi-temporal imagery using PCA, Hydrol. Process., 31, 800–810, 2017.

Allred, B. W., Fuhlendorf, S. D., Engle, D. M., and Elmore, R. D.: Ungulate preference for burned patches reveals strength of fire-grazing interaction, Ecol. Evol., 1, 132–144, https://doi.org/10.1002/ece3.12, 2011.

Arieira, J., Karssenberg, D., De Jong, S. M., Addink, E. A., Couto, E. G., Nunes Da Cunha, C., and Skøien, J. O.: Integrating field sampling, geostatistics and remote sensing to map wetland vegetation in the Pantanal, Brazil, 8, 667–686,
610 https://doi.org/10.5194/bg-8-667-2011, 2011.

Arscott, D. B., Tockner, K., Van Der Nat, D., and Ward, J. V: Aquatic habitat dynamics along a braided alpine river ecosystem (Tagliamento River, Northeast Italy), 5, 802–814, https://doi.org/10.1007/s10021-002-0192-7, 2002.

Basumatary, H., Devi, H. S., Borah, S. B., and Das, A. K.: Land cover dynamics and their driving factors in a protected floodplain ecosystem, River Res. Appl., 37, 627–643, https://doi.org/10.1002/rra.3775, 2021.

615 Beeri, O., Phillips, R., Hendrickson, J., Frank, A. B., and Kronberg, S.: Estimating forage quantity and quality using aerial hyperspectral imagery for northern mixed-grass prairie, Remote Sens. Environ., 110, 216–225, https://doi.org/10.1016/j.rse.2007.02.027, 2007.

Belgiu, M. and Drăgu, L.: Random forest in remote sensing: A review of applications and future directions, https://doi.org/10.1016/j.isprsjprs.2016.01.011, 1 April 2016.

620 Bhatta, S., Joshi, L. R., and Shrestha, B. B.: Distribution and impact of invasive alien plant species in Bardia National Park, western Nepal, Environ. Conserv., 47, 197–205, https://doi.org/10.1017/S0376892920000223, 2020.

Bhatta, S. R.: Status paper of Royal Bardia National Park, Grassl. Ecol. Manag. Prot. areas Nepal. Kathmandu ICIMOD, 122–127, 2000.

Bhattarai, B. P. and Kindlmann, P.: Habitat heterogeneity as the key determinant of the abundance and habitat preference of prey species of tiger in the Chitwan National Park, Nepal, Acta Theriol. (Warsz)., 57, 89–97, https://doi.org/10.1007/s13364-011-0047-8, 2012.

Bhattarai, B. R., Wright, W., Poudel, B. S., Aryal, A., Yadav, B. P., and Wagle, R.: Shifting paradigms for Nepal's protected areas: history, challenges and relationships, J. Mt. Sci., 14, 964–979, https://doi.org/10.1007/s11629-016-3980-9, 2017.

Biswas, T.: A spatio-temporal analysis of landscape change within the Eastern Terai, India: linking grassland and forest loss to change in river course and land use. PhD thesis, Utah State University, 2010.

Biswas, T., Ramsey, R. D., Bissonette, J. A., and Symanzik, J.: Integration of two spectral indices to monitor loss of moist grasslands within the Jaldapara Wildlife Sanctuary, India, Int. J. Remote Sens., 35, 1038–1063, https://doi.org/10.1080/01431161.2013.875631, 2014.

Bolton, M.: Royal Karnali Wildlife Reserve Management Plan, National P., FAO/UNDP, Rome, 70 pp., 1976.

Bond, W. J.: What limits trees in C4 grasslands and savannas?, https://doi.org/10.1146/annurev.ecolsys.39.110707.173411, 2008.

Bond, W. J. and Parr, C. L.: Beyond the forest edge: Ecology, diversity and conservation of the grassy biomes, Biol. Conserv., 143, 2395–2404, https://doi.org/10.1016/j.biocon.2009.12.012, 2010.

Breiman, L.: Random forests, Mach. Learn., 45, 5–32, https://doi.org/10.1023/A:1010933404324, 2001.

Brown, D. E. and Makings, E.: A guide to North American grasslands, University of Arizona for the Boyce Thompson Southwestern Arboretum, 2014.

Brown, K.: Plain tales from the grasslands: extraction, management and conservation of natural resources in Royal Bardia National Park, Nepal, Work. Pap. - Cent. Soc. Econ. Res. Glob. Environ., 1995.

Brown, K.: The political ecology of biodiversity, conservation and development in Nepal's Terai: Confused meanings, means and ends, Ecological Economics, 73–87 pp., 1998.

Buisson, E., Le Stradic, S., Silveira, F. A. O., Durigan, G., Overbeck, G. E., Fidelis, A., Fernandes, G. W., Bond, W. J., Hermann, J. M., Mahy, G., Alvarado, S. T., Zaloumis, N. P., and Veldman, J. W.: Resilience and restoration of tropical and subtropical grasslands, savannas, and grassy woodlands, Biol. Rev., 94, 590–609, https://doi.org/10.1111/brv.12470, 2019.

Chetri, M., Odden, M., and Wegge, P.: Snow leopard and Himalayan wolf: Food habits and prey selection in the central Himalayas, Nepal, PLoS One, 12, https://doi.org/10.1371/journal.pone.0170549, 2017.

Chhetri, T. B., Dhital, Y. P., Tandong, Y., Devkota, L. P., and Dawadi, B.: Observations of heavy rainfall and extreme flood events over Banke-Bardiya districts of Nepal in 2016–2017, Prog. Disaster Sci., 6, 100074, https://doi.org/10.1016/j.pdisas.2020.100074, 2020.

Clements, F. E.: Plant succession; an analysis of the development of vegetation, Plant succession; an analysis of the development of vegetation, Carnegie Institution of Washington, 1–512 pp., https://doi.org/10.5962/bhl.title.56234, 1916.

Corenblit, D., Tabacchi, E., Steiger, J., and Gurnell, A. M.: Reciprocal interactions and adjustments between fluvial landforms and vegetation dynamics in river corridors: A review of complementary approaches, Earth-Science Rev., 84, 56–86, https://doi.org/10.1016/j.earscirev.2007.05.004, 2007.

Corenblit, D., Steiger, J., and Tabacchi, E.: Biogeomorphologic succession dynamics in a Mediterranean river system, Ecography (Cop.)., 33, 1136–1148, https://doi.org/10.1111/j.1600-0587.2010.05894.x, 2010.

Crist, E. P. and Cicone, R. C.: Application of the Tasseled Cap concept to simulated Thematic Mapper data., Photogramm. Eng. Remote Sens., 50, 343–352, 1984.

665   Dahal, P., Shrestha, M. L., Panthi, J., and Pradhananga, D.: Modeling the future impacts of climate change on water availability in the Karnali River Basin of Nepal Himalaya, Environ. Res., 185, 109430, https://doi.org/10.1016/j.envres.2020.109430, 2020.

Dhakal, M., Karki, M., Jnawali, S. R., Subedi, N., Pradhan, N. M. B., Malla, S., Lamichhane, B. R., Pokheral, C. P., Thapa, G. J., and Oglethorpe, J.: Status of tigers and prey in Nepal, Dep. Natl. Park. Wildl. Conserv. Kathmandu, Nepal, 2014.

670   DHM: Observed climate trend analysis of Nepal in the districts and physiographic regions of Nepal (1971-2014), Dep. Hydrol. Meteorol. Nepal, 101, 2017.

Dinerstein, E.: An ecological survey of the royal Karnali-Bardia Wildlife Reserve, Nepal. Part I: Vegetation, modifying factors, and successional relationships, Biol. Conserv., 15, 127–150, https://doi.org/10.1016/0006-3207(79)90030-2, 1979a.

Dinerstein, E.: An ecological survey of the royal Karnali-Bardia Wildlife Reserve, Nepal. Part II: Habitat/Animal Interactions,
675   Biol. Conserv., 15, 127–150, https://doi.org/10.1016/0006-3207(79)90030-2, 1979b.

Dinerstein, E.: An ecological survey of the Royal Karnali-Bardia Wildlife Reserve, Nepal. Part III: Ungulate populations, Biol. Conserv., 18, 5–37, https://doi.org/10.1016/0006-3207(80)90063-4, 1980.

Dinerstein, E.: Effects of *Rhinoceros unicornis* on Riverine Forest Structure in Lowland Nepal, Source: Ecology, 701–704 pp., 1992.

680   Dingle, E., Attal, M., and Sinclair, H. D.: Abrasion-set limits on Himalayan gravel flux, https://doi.org/10.1038/nature22039, 2017.

Dingle, E. H., Creed, M. J., Sinclair, H. D., Gautam, D., Gourmelen, N., Borthwick, A. G. L., and Attal, M.: Dynamic flood topographies in the Terai region of Nepal, Earth Surf. Process. Landforms, 45, 3092–3102, https://doi.org/10.1002/esp.4953, 2020a.

685   Dingle, E. H., Sinclair, H. D., Venditti, J. G., Attal, M., Kinnaird, T. C., Creed, M., Quick, L., Nittrouer, J. A., and Gautam, D.: Sediment dynamics across gravel-sand transitions: Implications for river stability and floodplain recycling, Geology, 48, 468–472, https://doi.org/10.1130/G46909.1, 2020b.

DNPWC and DFSC: Status of Tigers and Prey in Nepal. Department of National Parks and Wildlife Conservation & Department of Forests and Soil Conservation. Ministry of Forests and Environment, 2018.

690   DNPWC and DFSC: Status of Tigers and Prey in Nepal. Department of National Parks and Wildlife Conservation & Department of Forests and Soil Conservation. Ministry of Forests and Environment, 2022.

Donchyts, G., Baart, F., Winsemius, H., Gorelick, N., Kwadijk, J., and Van De Giesen, N.: Earth's surface water change over the past 30 years, https://doi.org/10.1038/nclimate3111, 25 August 2016.

Dufour, S., Rinaldi, M., Piégay, H., and Michalon, A.: How do river dynamics and human influences affect the landscape
695   pattern of fluvial corridors? Lessons from the Magra River, Central-Northern Italy, Landsc. Urban Plan., 134, 107–118, https://doi.org/10.1016/j.landurbplan.2014.10.007, 2015.

Dufour, S., Rodríguez-González, P. M., and Laslier, M.: Tracing the scientific trajectory of riparian vegetation studies: Main topics, approaches and needs in a globally changing world, Sci. Total Environ., 653, 1168–1185, https://doi.org/10.1016/j.scitotenv.2018.10.383, 2019.

700   FAO: Map accuracy assessment and area estimation: a practical guide, Natl. For. Monit. Assess. Work. Pap., E, 69, 2016.

Filla, M., Lama, R. P., Ghale, T. R., Signer, J., Filla, T., Aryal, R. R., Heurich, M., Waltert, M., Balkenhol, N., and Khorozyan, I.: In the shadows of snow leopards and the Himalayas: density and habitat selection of blue sheep in Manang, Nepal, Ecol. Evol., 11, 108–122, https://doi.org/10.1002/ece3.6959, 2021.

Flannigan, M. D. and Wotton, B. M.: Climate, weather, and area burned, in: Forest Fires, Elsevier, 351–373,
705   https://doi.org/10.1016/b978-012386660-8/50012-x, 2001.

Ghimire, B., Bhujel, K., and Rijal, K.: Fire hazard zonation of Bardia National Park, Nepal: A disaster preparedness approach, Nepal J. Environ. Sci., 2, 27–33, https://doi.org/10.3126/njes.v2i0.22738, 2014.

Gómez, C., White, J. C., and Wulder, M. A.: Optical remotely sensed time series data for land cover classification: A review, ISPRS J. Photogramm. Remote Sens., 116, 55–72, https://doi.org/10.1016/j.isprsjprs.2016.03.008, 2016.

710 Gorelick, N., Hancher, M., Dixon, M., Ilyushchenko, S., Thau, D., and Moore, R.: Google Earth Engine: Planetary-scale geospatial analysis for everyone, Remote Sens. Environ., 202, 18–27, https://doi.org/10.1016/j.rse.2017.06.031, 2017.

Gu, Y., Brown, J. F., Verdin, J. P., and Wardlow, B.: A five-year analysis of MODIS NDVI and NDWI for grassland drought assessment over the central Great Plains of the United States, Geophys. Res. Lett., 34, https://doi.org/10.1029/2006GL029127, 2007.

715 Gumbel, E. J.: Statistics of extremes, Columbia university press, 1958.

Gunderson, L. H.: Panarchy: understanding transformations in human and natural systems, Island press, 2002.

Hansen, M. C. and Loveland, T. R.: A review of large area monitoring of land cover change using Landsat data, Remote Sens. Environ., 122, 66–74, https://doi.org/10.1016/j.rse.2011.08.024, 2012.

Harezlak, V., Geerling, G. W., Rogers, C. K., Penning, W. E., Augustijn, D. C. M., and Hulscher, S. J. M. H.: Revealing 35 720 years of land cover dynamics in floodplains of trained lowland rivers using satellite data, River Res. Appl., 1–9, https://doi.org/10.1002/rra.3633, 2020.

Harihar, A., Pandav, B., and MacMillan, D. C.: Identifying realistic recovery targets and conservation actions for tigers in a human-dominated landscape using spatially explicit densities of wild prey and their determinants, Divers. Distrib., 20, 567–578, https://doi.org/10.1111/ddi.12174, 2014.

725 Henderson-Sellers, A. and Pitman, A. J.: Land-surface schemes for future climate models: specification, aggregation, and heterogeneity, J. Geophys. Res., 97, 2687–2696, https://doi.org/10.1029/91JD01697, 1992.

Hermosilla, T., Wulder, M. A., White, J. C., Coops, N. C., and Hobart, G. W.: Disturbance-Informed Annual Land Cover Classification Maps of Canada's Forested Ecosystems for a 29-Year Landsat Time Series, Can. J. Remote Sens., 44, 67–87, https://doi.org/10.1080/07038992.2018.1437719, 2018.

730 Hirota, M., Holmgren, M., Van Nes, E. H., and Scheffer, M.: Global resilience of tropical forest and savanna to critical transitions, New Ser., 334, 232–235, https://doi.org/10.1126/science.l210465, 2011.

Hoetzel, S., Dupont, L., Schefuß, E., Rommerskirchen, F., and Wefer, G.: The role of fire in Miocene to Pliocene C4 grassland and ecosystem evolution, Nat. Geosci., 6, 1027–1030, https://doi.org/10.1038/ngeo1984, 2013.

Hupp, C. R. and Osterkamp, W. R.: Riparian vegetation and fluvial geomorphic processes, 14, 277–295, 735 https://doi.org/10.1016/0169-555X(95)00042-4, 1996.

Van Iersel, W. K., Addink, E. A., Straatsma, M. W., and Middelkoop, H.: River floodplain vegetation classification using multi-temporal high-resolution colour infrared UAV imagery, 2–5, https://doi.org/10.3990/2.423, 2016.

Van Iersel, W.: A bird's-eye view on river floodplains: Mapping and monitoring land cover with remote sensing. PhD thesis, Utrecht University, 2020.

740 Van Iersel, W., Straatsma, M., Addink, E., and Middelkoop, H.: Monitoring height and greenness of non-woody floodplain vegetation with UAV time series, ISPRS J. Photogramm. Remote Sens., 141, 112–123, https://doi.org/10.1016/j.isprsjprs.2018.04.011, 2018.

Iglesias, V., Whitlock, C., Markgraf, V., and Bianchi, M. M.: Postglacial history of the Patagonian forest/steppe ecotone (41-43°S), Quat. Sci. Rev., 94, 120–135, https://doi.org/10.1016/j.quascirev.2014.04.014, 2014.

745 Irengbam, M., Dobriyal, P., Hussain, S. A., and Badola, R.: Balancing conservation and development in Nandhaur Wildlife Sanctuary, Uttarakhand, India, Current Science, 2017.

Jalonen, J., Järvelä, J., Virtanen, J. P., Vaaja, M., Kurkela, M., and Hyyppä, H.: Determining characteristic vegetation areas by terrestrial laser scanning for floodplain flow modeling, 7, 420–437, https://doi.org/10.3390/w7020420, 2015.

Jnawali, S. R. and Wegge, P.: Importance of tall grasslands in megaherbivore conservation., in: Grassland ecology and management in protected areas of Nepal. Proceedings of a Workshop, Royal Bardia National Park, Thakurdwara, Bardia, Nepal, 15-19 March, 1999. Volume 2: Terai protected areas, 84–91, 2000.

Jnawali, S. R. and Wegge, P. W.: Space and habitat use by a small re-introduced population of greater one–horned rhinoceros in RBNP–a preliminary report, 1993.

Junk, W. J., Bayley, P. B., and Sparks, R. E.: The flood pulse concept in river-floodplain systems, Can. Spec. Publ. Fish. Aquat. Sci., 106, 110–127, 1989.

Karki, J. B., Jhala, Y. V., Pandav, B., Jnawali, S. R., Shrestha, R., Thapa, K., Thapa, G., Pradhan, N. M. B., Lamichane, B. R., and Barber-Meyer, S. M.: Estimating tiger and its prey abundance in Bardia National Park, Nepal, Banko Janakari, 26, 60–69, https://doi.org/10.3126/banko.v26i1.15503, 2016.

Kelley, L. C., Pitcher, L., and Bacon, C.: Using google earth engine to map complex shade-grown coffee landscapes in northern Nicaragua, Remote Sens., 10, https://doi.org/10.3390/rs10060952, 2018.

Kollmann, J., Vieli, M., Edwards, P. J., Tockner, K., and Ward, J. V.: Interactions between vegetation development and island formation in the Alpine river Tagliamento, Appl. Veg. Sci., 2, 25–36, https://doi.org/10.2307/1478878, 1999.

Kral, M. J. C., Van Lunenburg, M., and Van Alphen, J. J. M.: The spatial distribution of ungulates and primates across the vegetation gradient in Bardiya National Park, West Nepal, Asian J. Conserv. Biol., 6, 38–44, 2017.

Lallias-Tacon, S., Liébault, F., and Piégay, H.: Use of airborne LiDAR and historical aerial photos for characterising the history of braided river floodplain morphology and vegetation responses, 149, 742–759, https://doi.org/10.1016/j.catena.2016.07.038, 2017.

Van Langevelde, F., Van De Vijver, C. A. D. M., Kumar, L., Van De Koppel, J., De Ridder, N., Van Andel, J., Skidmore, A. K., Hearne, J. W., Stroosnijder, L., Bond, W. J., Prins, H. H. T., and Rietkerk, M.: Effects of fire and herbivory on the stability of savanna ecosystems, Ecology, 84, 337–350, https://doi.org/10.1890/0012-9658, 2003.

Lawrence, R. L., Wood, S. D., and Sheley, R. L.: Mapping invasive plants using hyperspectral imagery and Breiman Cutler classifications (RandomForest), Remote Sens. Environ., 100, 356–362, https://doi.org/10.1016/j.rse.2005.10.014, 2006.

Lehmann, C. E. R., Anderson, T. M., Sankaran, M., Higgins, S. I., Archibald, S., Hoffmann, W. A., Hanan, N. P., Williams, R. J., Fensham, R. J., Felfili, J., Hutley, L. B., Ratnam, J., San Jose, J., Montes, R., Franklin, D., Russell-Smith, J., Ryan, C. M., Durigan, G., Hiernaux, P., Haidar, R., Bowman, D. M. J. S., and Bond, W. J.: Savanna vegetation-fire-climate relationships differ among continents, Science (80-.)., 343, 548–552, https://doi.org/10.1126/science.1247355, 2014.

Lehmkuhl, J.: The ecology of south-Asian tall-grass communities, PhD dissertation, University of Washington, Seattle, WA, 1989.

Lehmkuhl, J. F.: A classification of subtropical riverine grassland and forest in Chitwan National Park, Nepal, 111, 29–43, https://doi.org/10.1007/BF00045575, 1994.

Lehmkuhl, J. F.: The organisation and human use of Terai riverine grasslands in the Royal Chitwan National Park, Nepal., Grassl. Ecol. Manag. Prot. areas Nepal. Proc. a Work. R. Bardia Natl. Park. Thakurdwara, Bardia, Nepal, 15-19 March, 1999. Vol. 2 Terai Prot. areas, 37–49, 2000.

Leier, A. L., DeCelles, P. G., and Pelletier, J. D.: Mountains, monsoons, and megafans, Geology, 33, 289–292, https://doi.org/10.1130/G21228.1, 2005.

Lorenz, C. M., Dijk, G. M. Van, Hattum, A. G. M. Van, and Cofino, W. P.: Concepts in river ecology: implications for indicator development, Regul. Rivers Res. Manag., 13, 501–516, https://doi.org/10.1002/(SICI)1099-1646(199711/12)13:6<501::AID-RRR479>3.0.CO;2-1, 1997.

790 Louzada, R. O., Bergier, I., and Assine, M. L.: Landscape changes in avulsive river systems: Case study of Taquari River on Brazilian Pantanal wetlands, Sci. Total Environ., 723, 138067, https://doi.org/10.1016/j.scitotenv.2020.138067, 2020.

van Lunenburg, M., Kral, M. J. C., and van Alphen, J. J. M.: Decreased ungulate density in Bardiya National Park, West Nepal, and the implications for increasing tiger populations. A comment on Thapa et al. (2015), https://doi.org/10.1080/03949370.2016.1145147, 4 May 2017.

795 Lyngdoh, S., Shrotriya, S., Goyal, S. P., Clements, H., Hayward, M. W., and Habib, B.: Prey preferences of the snow leopard (*Panthera uncia*): Regional diet specificity holds global significance for conservation, PLoS One, 9, https://doi.org/10.1371/journal.pone.0088349, 2014.

MacClune, K., Yadav, S., Venkateswaran, K., Maharjan, R., Dixit, K. M., and Dugar, S.: Urgent case of recovery: what we can learn from the August 2014 Karnali River floods in Nepal, 2014.

800 Mas, J. F. and Vega, E.: Assessing yearly transition probability matrix for land use/land cover dynamics, Accuracy 2012 - Proc. 10th Int. Symp. Spat. Accuracy Assess. Nat. Resour. Environ. Sci., 345–350, 2012.

McGarigal, K. ;Cushma.: FRAGSTATS: Spatial pattern analysis program for categorical maps. Computer software program produced by the authors at the University of Massachusetts, Amherst. http://www.umass.edu/landeco/research/fragstats/fragstats.html, 2002.

805 McGarigal, K. and Marks, B. J.: FRAGSTATS: spatial pattern analysis program for quantifying landscape structure, General Technical Report - US Department of Agriculture, Forest Service, 128 pp., 1995.

Meyer, W. B. and Turner, B. L.: Human population growth and global land-use/cover change, II Source: Annual Review of Ecology and Systematics, 39–61 pp., 1992.

Moe, S. R. and Wegge, P.: Spacing behaviour and habitat use of axis deer (*Axis axis*) in lowland Nepal, Can. J. Zool., 72, 810 1735–1744, https://doi.org/10.1139/z94-234, 1994.

Myneni, R. B., Hall, F. G., Sellers, P. J., and Marshak, A. L.: Interpretation of spectral vegetation indexes, IEEE Trans. Geosci. Remote Sens., 33, 481–486, https://doi.org/10.1109/36.377948, 1995.

Neupane, D., Kwon, Y., Risch, T. S., and Johnson, R. L.: Changes in habitat suitability over a two decade period before and after Asian elephant recolonization, Glob. Ecol. Conserv., 22, https://doi.org/10.1016/j.gecco.2020.e01023, 2020.

815 Newbold, C. and Mountford, O.: Water level requirements of wetland plants and animals, English Nature, 1997.

Odden, M.: Tigers, leopards and their prey in Bardia National Park, Nepal. PhD thesis, Norwegian University of Life Sciences, https://doi.org/10.13140/RG.2.2.29496.75527, 2007.

Odden, M. and Wegge, P.: Spacing and activity patterns of leopards *Panthera pardus* in the Royal Bardia National Park, Nepal, Wildlife Biol., 11, 145–152, https://doi.org/10.2981/0909-63962005.

820 Odden, M., Wegge, P., and Storaas, T.: Hog deer (Axis porcinus) need threatened tallgrass floodplains: A study of habitat selection in lowland Nepal, Anim. Conserv., 8, 99–104, https://doi.org/10.1017/S1367943004001854, 2005.

Oli, M. K.: Seasonal patterns in habitat use of blue sheep *Pseudois nayaur* (Artiodactyla, Bovidae) in Nepal, Mammalia, 60, 187–193, https://doi.org/10.1515/mamm.1996.60.2.187, 1996.

Orem, C. A. and Pelletier, J. D.: Quantifying the time scale of elevated geomorphic response following wildfires using multi-825 temporal LiDAR data: An example from the Las Conchas fire, Jemez Mountains, New Mexico, 232, 224–238, https://doi.org/10.1016/j.geomorph.2015.01.006, 2015.

Owen-Smith, R. N.: Megaherbivores: the influence of very large body size on ecology, Cambridge university press, 1988.

Pal, M.: Random forest classifier for remote sensing classification, Int. J. Remote Sens., 26, 217–222, https://doi.org/10.1080/01431160412331269698, 2005.

830 Parr, C. L., Gray, E. F., and Bond, W. J.: Cascading biodiversity and functional consequences of a global change-induced biome switch, Divers. Distrib., 18, 493–503, https://doi.org/10.1111/j.1472-4642.2012.00882.x, 2012.

Peet, N. B.: Biodiversity and the management of tall grassland in Nepal. PhD thesis, University of East Anglia, 1997.

Peet, N. B., Watkinson, A. R., Bell, D. J., and Kattel, B. J.: Plant diversity in the threatened sub-tropical grasslands of Nepal, Biol. Conserv., 88, 193–206, https://doi.org/10.1016/S0006-3207(98)00104-9, 1999a.

835 Peet, N. B., Watkinson, A. R., Bell, D. J., and Sharma, U. R.: The conservation management of Imperata cylindrica grassland in Nepal with fire and cutting: An experimental approach, J. Appl. Ecol., 36, 374–387, https://doi.org/10.1046/j.1365-2664.1999.00405.x, 1999b.

Pickett, S. T. A., Collins, S. L., and Armesto, J. J.: A hierarchical consideration of causes and mechanisms of succession, in: Theory and models in vegetation science, Springer, 109–114, 1987.

840 Plakman, V., Janssen, T., Brouwer, N., and Veraverbeke, S.: Mapping species at an individual-tree scale in a temperate forest, using Sentinel-2 images, airborne laser scanning data, and random forest classification, Remote Sens., 12, 1–25, https://doi.org/10.3390/rs12223710, 2020.

Plexida, S. G., Sfougaris, A. I., Ispikoudis, I. P., and Papanastasis, V. P.: Selecting landscape metrics as indicators of spatial heterogeneity-A comparison among Greek landscapes, Int. J. Appl. Earth Obs. Geoinf., 26, 26–35,
845 https://doi.org/10.1016/j.jag.2013.05.001, 2014.

Poff, N. L., Allan, J. D., Bain, M. B., Karr, J. R., Prestegaard, K. L., Richter, B. D., Sparks, R. E., and Stromberg, J. C.: The natural flow regime, Bioscience, 47, 769–784, 1997.

Pokheral, S. K.: Floristic composition, biomass production, and biomass harvest in the grasslands of the Royal Bardia National Park, Bardia, Nepal, M.Sc. thesis, Agric. Univ. Norw., 1993.

850 Pradhan, N. M. B., Wegge, P., Moe, S. R., and Shrestha, A. K.: Feeding ecology of two endangered sympatric megaherbivores: Asian elephant *Elephas maximus* and greater one-horned rhinoceros *Rhinoceros unicornis* in lowland Nepal, Wildlife Biol., 14, 147–154, https://doi.org/10.2981/0909-6396(2008)14[147:FEOTES]2.0.CO;2, 2008.

Price, K. P., Guo, X., and Stiles, J. M.: Optimal landsat TM band combinations and vegetation indices for discrimination of six grassland types in eastern Kansas, Int. J. Remote Sens., 23, 5031–5042,
855 https://doi.org/10.1080/01431160210121764, 2002.

Rakhal, B., Adhikari, T. R., Sharma, S., and Ghimire, G. R.: Assessment of channel shifting of Karnali Megafan in Nepal using remote sensing and GIS, Ann. GIS, https://doi.org/10.1080/19475683.2021.1871950, 2021.

Ram, A. K. and Acharya, H.: Status distribution and habitat use by Asian elephants in Nepal, A Compend. Conserv. Bulletien, 155–160, 2020.

860 Rapinel, S., Mony, C., Lecoq, L., Clément, B., Thomas, A., and Hubert-Moy, L.: Evaluation of Sentinel-2 time-series for mapping floodplain grassland plant communities, Remote Sens. Environ., 223, 115–129, https://doi.org/10.1016/j.rse.2019.01.018, 2019.

Rock, B. N., Vogelmann, J. E., Williams, D. L., Vogelmann, A. F., and Hoshizaki, T.: Remote Detection of Forest Damage, Bioscience, 36, 439–445, https://doi.org/10.2307/1310339, 1986.

865 Rouse, J. W., Hass, R. H., Schell, J. A., and Deering, D. W.: Monitoring vegetation systems in the great plains with ERTS, Third Earth Resources Technology Satellite (ERTS) symposium, 309–317 pp., https://doi.org/citeulike-article-id:12009708, 1973.

Rovero, F., Augugliaro, C., Havmoller, R. W., Groff, C., Zimmermann, F., Oberosler, V., and Tenan, S.: Co-occurrence of snow leopard *Panthera uncia*, Siberian ibex *Capra sibirica* and livestock: Potential relationships and effects, 54, 118–124, https://doi.org/10.1017/S0030605317001685, 2020.

870

Roy, D. P., Kovalskyy, V., Zhang, H. K., Vermote, E. F., Yan, L., Kumar, S. S., and Egorov, A.: Characterization of Landsat-7 to Landsat-8 reflective wavelength and normalized difference vegetation index continuity, Remote Sens. Environ., 185, 57–70, https://doi.org/10.1016/j.rse.2015.12.024, 2016.

Sankaran, M.: Diversity patterns in savanna grassland communities: Implications for conservation strategies in a biodiversity

875

hotspot, Biodivers. Conserv., 18, 1099–1115, https://doi.org/10.1007/s10531-008-9519-9, 2009.

Sarma, P. K., Lahkar, B. P., Ghosh, S., Rabha, A., Das, J. P., Nath, N. K., Dey, S., and Brahma, N.: Land-use and land-cover change and future implication analysis in Manas National Park, India using multi-temporal satellite data, Curr. Sci., 95, 223–227, 2008.

Seidensticker, J.: Ungulate populations in Chitawan Valley, Nepal, Biol. Conserv., 10, 183–210, https://doi.org/10.1016/0006-

880

3207(76)90034-3, 1976.

Sertel, E., Topaloğlu, R. H., Şallı, B., Algan, I. Y., and Aksu, G. A.: Comparison of landscape metrics for three different level land cover/land use maps, ISPRS Int. J. Geo-Information, 7, https://doi.org/10.3390/ijgi7100408, 2018.

Sharma, B. K.: Wildlife habitat mapping by using Geographic Information Systems (GIS) in the Karnali floodplain of Royal Bardia National Park in lowland Nepal. M.Sc. thesis, Norwegian University of Life Sciences., 1999.

885

Shrestha, S. and Shrestha, J.: Asian elephants and their status in Nepal: a review, J. Agric. Nat. Resour., 4, 227–237, https://doi.org/10.3126/janr.v4i2.33828, 2021.

Sinclair, H. D., Brown, S., Adhikari, B. R., Attal, M., Borthwick, A., Budimir, M., Creed, M., Dingle, E. H., Dugar, S., Gautam, D., Gourmelen, N., Mudd, S. M., Neupane, S., Pedreschi, R., Ruwanpura, K. N., Sharma, J., Sneddon, A., and Uprety, M.: Improving understanding of flooding and resilience in the Terai, Nepal, 1–5, 2017.

890

Solins, J. P., Thorne, J. H., and Cadenasso, M. L.: Riparian canopy expansion in an urban landscape: Multiple drivers of vegetation change along headwater streams near Sacramento, California, https://doi.org/10.1016/j.landurbplan.2017.12.005, 2017.

Staver, A. C., Archibald, S., and Levin, S. A.: The global extent and determinants of savanna and forest as alternative biome states, Science (80-.)., 334, 230–232, https://doi.org/10.1126/science.1210465, 2011.

895

Straatsma, M. W. and Baptist, M. J.: Floodplain roughness parameterization using airborne laser scanning and spectral remote sensing, Remote Sens. Environ., 112, 1062–1080, https://doi.org/10.1016/j.rse.2007.07.012, 2008.

Takahata, C., Amin, R., Sarma, P., Banerjee, G., Oliver, W., and Fa, J. E.: Remotely-sensed active fire data for protected area management: Eight-year patterns in the Manas National Park, India, Environ. Manage., 45, 414–423, https://doi.org/10.1007/s00267-009-9411-8, 2010.

900

Thapa, K., Nepal, S., Thapa, G., Bhatta, S. R., and Wikramanayake, E.: Past, present and future conservation of the greater one-horned rhinoceros *Rhinoceros unicornis* in Nepal, 47, 345–351, https://doi.org/10.1017/S0030605311001670, 2013.

Thapa, S. K., de Jong, J. F., Subedi, N., Hof, A. R., Corradini, G., Basnet, S., and Prins, H. H. T.: Forage quality in grazing lawns and tall grasslands in the subtropical region of Nepal and implications for wild herbivores, Glob. Ecol. Conserv.,

905

30, e01747, https://doi.org/10.1016/j.gecco.2021.e01747, 2021.

Thapa, T. B.: Habitat Suitability Evaluation for Leopard (*Panthera pardus*) Using Remote Sensing and GIS in and Around Chitwan National Park, Nepal. PhD thesis, Saurashtra University, 2011.

Thing, S. J., Jones, R., and Jones, C. B.: The Politics of Conservation: Sonaha, Riverscape in the Bardia National Park and Buffer Zone, Nepal, Conserv. Soc., 15, 292–303, https://doi.org/10.4103/cs.cs_15_2, 2017.

910 Thorne, C. R., Russell, A. P. G., and Alam, M. K.: Planform pattern and channel evolution of the Brahmaputra River, Bangladesh, Geol. Soc. Spec. Publ., 75, 257–276, https://doi.org/10.1144/GSL.SP.1993.075.01.16, 1993.

Tilman, D.: Plant strategies and the dynamics and structure of plant communities Princeton, New Jersey Princet. Univ. Press, 26–28, 1988.

Trauernicht, C., Murphy, B. P., Tangalin, N., and Bowman, D. M. J. S.: Cultural legacies, fire ecology, and environmental 915 change in the Stone Country of Arnhem Land and Kakadu National Park, Australia, Ecol. Evol., 3, 286–297, https://doi.org/10.1002/ece3.460, 2013.

Turner, M. G., Baker, W. L., Peterson, C. J., and Peet, R. K.: Factors influencing succession: Lessons from large, infrequent natural disturbances, 1, 511–523, https://doi.org/10.1007/s100219900047, 1998.

USAID: Lower Karnali Watershed Health Report, 1–23, 2018.

920 Veldman, J. W., Buisson, E., Durigan, G., Fernandes, G. W., Le Stradic, S., Mahy, G., Negreiros, D., Overbeck, G. E., Veldman, R. G., Zaloumis, N. P., Putz, F. E., and Bond, W. J.: Toward an old-growth concept for grasslands, savannas, and woodlands, https://doi.org/10.1890/140270, 1 April 2015.

Vesipa, R., Camporeale, C., and Ridolfi, L.: Effect of river flow fluctuations on riparian vegetation dynamics: Processes and models, Adv. Water Resour., 110, 29–50, https://doi.org/10.1016/j.advwatres.2017.09.028, 2017.

925 Wagner-Lücker, I., Lanz, E., Förster, M., Janauer, G. A., and Reiter, K.: Knowledge-based framework for delineation and classification of ephemeral plant communities in riverine landscapes to support EC Habitat Directive assessment, Ecol. Inform., 14, 44–47, https://doi.org/10.1016/j.ecoinf.2012.11.003, 2013.

Wang, J., Wang, K., Zhang, M., and Zhang, C.: Impacts of climate change and human activities on vegetation cover in hilly southern China, Ecol. Eng., 81, 451–461, https://doi.org/10.1016/j.ecoleng.2015.04.022, 2015.

930 Wegge, P. and Storaas, T.: Sampling tiger ungulate prey by the distance method: Lessons learned in Bardia National Park, Nepal, Anim. Conserv., 12, 78–84, https://doi.org/10.1111/j.1469-1795.2008.00230.x, 2009.

Wegge, P., Odden, M., and Storaas, T.: No decline in ungulate prey for tigers in Bardia National Park in Nepal: comments on van Lunenburg et al. (2017) and Kral et al. (2017), https://doi.org/10.1080/03949370.2019.1609094, 2019.

White, P. S.: Natural disturbance and patch dynamics: an introduction, Nat. Disturb. patch Dyn., 3–13, 1985.

935 White, R. P., Murray, S., Rohweder, M., Prince, S. D., and Thompson, K. M.: Grassland ecosystems, World Resources Institute Washington, DC, USA, 2000.

Young, N. E., Anderson, R. S., Chignell, S. M., Vorster, A. G., Lawrence, R., and Evangelista, P. H.: A survival guide to Landsat preprocessing, Ecology, 98, 920–932, https://doi.org/10.1002/ecy.1730, 2017.

Zanter, K.: Landsat Collection 1 Level 1 Product Definition. United States Geological Survey., United States Geological 940 Survey, 26 pp., 2019.

Zhu, Z., Wang, S., and Woodcock, C. E.: Improvement and expansion of the Fmask algorithm: Cloud, cloud shadow, and snow detection for Landsats 4-7, 8, and Sentinel 2 images, Remote Sens. Environ., 159, 269–277, https://doi.org/10.1016/j.rse.2014.12.014, 2015.

Zurqani, H. A., Post, C. J., Mikhailova, E. A., Schlautman, M. A., and Sharp, J. L.: Geospatial analysis of land use change in 945 the Savannah River Basin using Google Earth Engine, Int. J. Appl. Earth Obs. Geoinf., 69, 175–185, https://doi.org/10.1016/j.jag.2017.12.006, 2018.

Appendices

965 **Appendix A: Overview of anthropogenic activities in BNP as recorded in literature**

Year	Activity	Description	Source
1925	Commercial forestry	5 years of extensive deforestation.	Bolton (1976)
Since 1950	Increase of population	Increased deforestation and pressure on forest.	Brown (1997) and Bhatterai et al. (2017)
1965-1975	Possible cultivation of Baghaura and Lamkauli phantas	Oral records deliver cultivation of these phantas.	Dinerstein (1979a) and Pokharel (1993)
1976	Free access for locals refused and livestock grazing was prohibited.	Establishment as conservation area: The Royal Bardia Wildlife Reserve (348 km^2)	Bhatta (2000)
1978-1994	Management practices	Controlled burning in phantas. Ploughing, introduction of grass species and uprooting of stumps from 1978 to 1994 on the Baghaura phanta for the reintroduced black buck (*Antilope cervicapra*)	Bhatta (2000)
1979	Resource collection allowed, 7 days of access	Local communities were granted the rights to collect thatch grass and reeds from the reserves once a year, which was a pioneer step towards a people-centered approach.	Brown (1997)
1979-1983	Relocation of settlements	572 families were relocated from the Babai Valley of BNP.	Brown (1997)
1983	Registered permits: 21,081; 15 days of access	Permits were issued for entering the part for resource collection.	Bhatta (2000)
1994	Nr. of days for resource collection reduced to 10 days	-	Bhatta (2000)
1995	Uprooting at the Khauraha and Baghaura phanta	Uprooting of unpalatable species (*Lantana sp.* and *Colebrookia sp.*) as part of the Bardia Integrated Conservation Project (1995-2001). Extensive uprooting was executed on the Khauraha phanta in 1999.	Bhatta (2000)
1999	Registered permits: 57,255 Extensive uprooting of small bushes and trees at Khauraha phanta	Gradual increase of permits from 21k (1983) to 57k (1999)	Bhatta (2000)
2020	Nr. of days for resource collection is 3 days, drastical decrease of permits (number unknown)	-	Thapa et al. (2021)

To establish an annual time series of land cover, we selected imagery of the Surface Reflectance dataset (Tier 1) of LANDSAT 5, 7 and 8 satellites between 1993 and 2019. This dataset of imagery is corrected for variation of the energy source (e.g. sun angle) and atmospheric effects (e.g. aerosol scattering and thin clouds) and is therefore best suited to use for diachronic analysis

970 (Zanter, 2019; Young et al., 2017). We accounted for the differences in sensors by using coefficients (Roy et al., 2016) to correct LANDSAT OLI imagery to LANDSAT 7 ETM+ imagery. The incorporation of seasonal information improves the classification results, especially if height data is absent, as the spectral signatures of the separate classes are more distinct due to phenological differences of vegetation throughout the year (Van Iersel et al., 2016; Kelley et al., 2018). For each year, two separate collections of images were selected based on the day of the year (between 240-366 of the post-monsoon and 1-150 of

975 the subsequent pre-monsoon). In addition, images were selected based on cloud cover (< 50 %), quality (> 9), geometric RMSE (Root Mean Square Error) of < 10 m and we performed cloud masking using the *Fmask* algorithm (Zhu et al., 2015). To enhance the available spectral information, NDVI (Rouse et al., 1973; Rock et al., 1986; Myneni et al., 1995; Beeri et al., 2007), NDDI (Gu et al., 2007), and Tasseled Cap Transformations (Crist and Cicone, 1984) were calculated, which have been shown to improve classification results of vegetation (Price et al., 2002; Biswas, 2010). From each seasonal selection the

980 images were combined into a composite image by taking the median value of each seasonal collection. In addition, for each year a separate annual collection of images was created, which was used to calculate the seasonal variation of the NDVI metric with a harmonic trend for each pixel in terms of magnitude and timing of the annual change. This was added as indicator for the supervised classification model. To minimized noise caused by clouds, artifacts and the LANDSAT 7 Scan-line error we repeated the seasonal selection of imagery five times for each year with slightly different selection dates. After classification,

985 the modus of the resulting five land cover maps was taken to obtain the most prevailing classification for each pixel for each year. The composites of 1995, 1997 and 2006 were not classified. Too many clouds were present for 1995 and 1997 and a too large number of erroneous pixel values in the image composite was observed for 2006, caused by the LANDSAT 7 Scan-line error. We used *Google Earth Engine* (Gorelick et al., 2017), earlier applied for mapping changes in floodplain ecosystems (Harezlak et al., 2020; Zurqani et al., 2018; Donchyts et al., 2016; Van Iersel, 2020), for selecting, processing and classifying

990 LANDSAT imagery, whereas RStudio was used for post-classification analysis.

Appendix C: Grouping of vegetation types: Vegetation assemblages present in Bardia National Park and its associated vegetation class as used in the Level 2 classification model in this study. Grass assemblages from Peet et al. (1999a). Forest assemblages are from Dinerstein (1979a) and modification of (Jnawali and Wegge, 1993; Pokheral, 1993).

995

Assemblage	Vegetation class (level 2)
Typha elephantina assemblage; permanently waterlogged sites	Alluvial tall grassland
Phragmites karka-Saccharum spontaneum assemblage; seasonally inundated, heavily grazed	Alluvial tall grassland
Phragmites karka-Saccharum spontaneum-Saccharum arundinaceum assemblage	Alluvial tall grassland
Phragmites karka assemblage; Tall, dense riverine grassland, seasonal and permanent marsh	Alluvial tall grassland
Saccharum spontaneum assemblage; Mixed *Saccharum spontaneum* phase, *Saccharum spontaneum* phase, *Saccharum spontaneum-Dalbergia sissoo* phase, floodplain grasslands, alluvial soils, often inundated	Alluvial tall grassland
Imperata cylindrica-Narenga porphyrocoma assemblage; (1) *Saccharum spontaneum-Saccharum bengalense* phase, edges of wet sites, newer river terraces. (2) *Imperata cylindrica* phase, sites where tall grasses invading an *Imperata cylindirica* dominated sward.	Alluvial tall grassland if (1) Mixed tall grassland if (2) and > 50 % is higher than 2 m Short grassland: if > 50 % is lower than 2 m
Imperata cylindrica assemblage; *Imperata cylindrica* phase, *Erianthus ravennae* phase; *Imperata-Saccharum* phase; dry sites, well developed	Short grassland: if > 50% is lower than 2 m, or Mixed tall grassland: if > 50 % is higher than 2 m

soils, previously cultivated		
Narenga porphyrocoma assemblage; Tall, dense grassland, older river terraces and wetter sites, influenced by fire	Mixed tall grassland	
Themeda arundinacea assemblage; Tall, dense grassland, often at forest edge, well developed soils, influenced by fire	Mixed tall grassland	
Sal forest	Sal forest	
Dry sal forest	Sal forest	
Hill sal forest	Sal forest	
Khair-Sissoo forest *(Dalbergia sissoo-Acacia catechu)*	Riverine forest	
Mixed hardwood forest (Ficus glomerata-Mallotus phillippinenis-Eugenia jambolana	Riverine forest	
Moist riverine forest *(Mallotus phillipinensis* and *Syzigium cumini)*	Riverine forest	

Appendix D: Dominant species per vegetation type used for assigning classes. Cover and height are used for further discrimination of classes.

Criteria	Mixed tall grasslands	Alluvial tall grasslands	Short grasslands	Sal forest	Riverine forest	Shrubland
Dominant species	*Narenga porphyrocoma, Themeda arundinacea, Erianthus ravennae, Bombax ceiba*	*Saccharum spontaneum, Phragmites karka, Saccharum arundinaceum*	*Imperata cylindrica, Vitiveria zizanioides, Desmostachyia bipinnata.*	*Shorea robusta, Terminalia tomentosa*	*Dalbergia sissoo, Acacia catechu, Mallotus phillippinensis, Syzigium cumini, Bombax ceiba, Lantana Camara*	-
Cover	> 50% grass	> 50% grass	> 50% short grass	> 50% trees	> 50% trees	> 50% shrubs
Height	> 2 m	> 2 m	< 2 m	> 5 m	> 5 m	< 5 m

1000

Appendix E: Confusion matrices of the level 1 and level 2 classifications for 2019, as calculated with 30% of the ground truth data and confusion matrices for 2000, 2010, 2011 and 2018 based on separate validation set (106 samples).

2019 Level 1	Forest	Grassland	Bare	Water	Sum	User's accuracy
Forest	38	5	0	0	43	88.4
Grassland	3	34	0	0	37	91.9
Bare	0	4	6	0	10	60.0
Water	1	1	1	5	8	62.5
Sum	42	44	7	5	98	
Producer's accuracy	90.5	77.3	85.7	100.0		**84.7%**

2019 Level 2	Sal forest	Alluvial tall grassland	Short grassland	Bare	Water	Shrubland	Riverine forest	Mixed tall grassland	Sum	User's accuracy
Sal forest	24	0	0	0	0	0	0	0	24	100.0
Wet tall grassland	0	8	1	1	0	0	0	0	10	80.0
Short grassland	0	1	14	1	0	0	0	1	17	82.4
Bare	0	3	1	11	0	0	0	0	15	73.3

									Sum	Producer's accuracy
Water	0	1	0	0	11	0	0	0	12	91.7
Shrubland	1	0	1	0	0	2	1	3	8	25.0
Riverine forest	1	0	1	1	0	0	13	0	16	81.3
Mixed tall grassland	0	1	6	0	0	1	1	5	14	35.7
Sum	26	14	24	14	11	3	15	9	116	
Producer's accuracy	92.3	57.1	78.6	78.6	100.0	66.7	86.7	55.6		**75.7%**

2000 Level 1	Forest	Grassland	Bare	Water	Sum	User's accuracy
Forest	45	4	0	0	49	91.8
Grassland	3	20	0	0	23	87.0
Bare	0	7	10	5	22	45.5
Water	1	4	2	5	12	41.7
Sum	49	35	12	10	106	
Producer's accuracy	91.8	57.1	83.3	50.0		**75.5%**
p-value	1.43E-07	**CI95**	0.66	0.83	**kappa**	0.64

2010 Level 1	Forest	Grassland	Bare	Water	Sum	User's accuracy
Forest	45	5	0	0	50	90.0
Grassland	1	14	0	0	15	93.3
Bare	1	1	22	5	29	75.9
Water	1	0	0	11	12	91.7
Sum	48	20	22	16	106	
Producer's accuracy	93.8	70.0	100.0	68.8		**86.8%**
p-value	3.06E-15	**CI95**	0.79	0.93	**kappa**	0.81

2011 Level 1	Forest	Grassland	Bare	Water	Sum	User's accuracy
Forest	45	6	0	0	51	88.2
Grassland	1	13	0	0	14	92.9
Bare	0	1	20	7	28	71.4
Water	0	0	1	12	13	92.3
Sum	46	20	21	19	106	
Producer's accuracy	97.8	65.0	95.2	63.2		**84.9%**
p-value	1.10E-13	**CI95**	0.77	0.91	**kappa**	0.78

2018 Level 1	Forest	Grassland	Bare	Water	Sum	User's accuracy
Forest	46	4	0	1	51	90.0
Grassland	5	20	1	1	27	74.0
Bare	0	5	10	4	19	52.6
Water	0	2	0	7	9	77.8
Sum	51	31	11	13	106	
Producer's accuracy	90.2	64.5	90.9	53.8		**78.3%**
p-value	3.78-e09	**CI95**	0.69	0.86	**kappa**	0.67

1005

Figure A1: View from tower (Bagh Machan). In the front *Saccharum spontaneum* dominated tall grasslands grow. Behind dryer types of grassland are present. At the right a patch of grassland is present that was cut short. Behind the grassland riverine forest is present. The location is northwest from the Khauraha phanta. As entering these grasslands is not recommended, this view is used to assign ground truth locations for short grassland, alluvial tall grassland (in front) and on the far end mixed tall grasslands and riverine forest. This was done in
1010 combination with satellite imagery to obtain the exact coordinates. Photograph taken by authors.

Figure A2: Sal forest on top and grasses below. At the right, tall grasses grow amongst the grasses classified as short grassland. The cliff
1015 marks the spatial extent of fluvial disturbances of the Karnali river. The difference in elevation is largest at the boundary between Sal and the floodplain in the northwest of the study area, and gradually decreases southwards along the interface of riverine forest and Sal forest. In the outcrop a loamy layer is positioned on top of a more sandy layer containing rounded pebbles, cobbles and boulders. Photograph taken by authors.

1020

Figure A3: Series of land cover maps of Level 1 and Level 2 classifications.
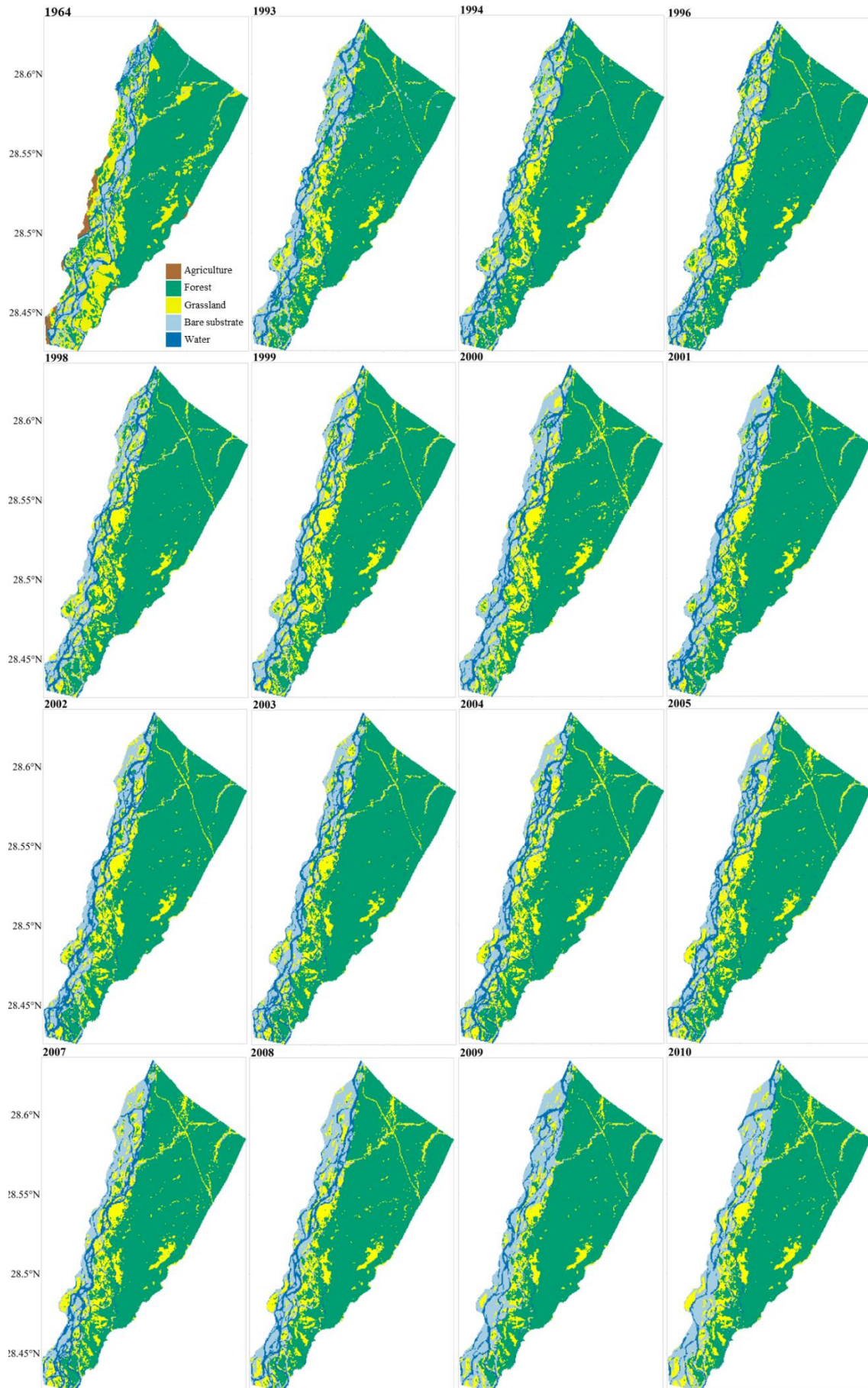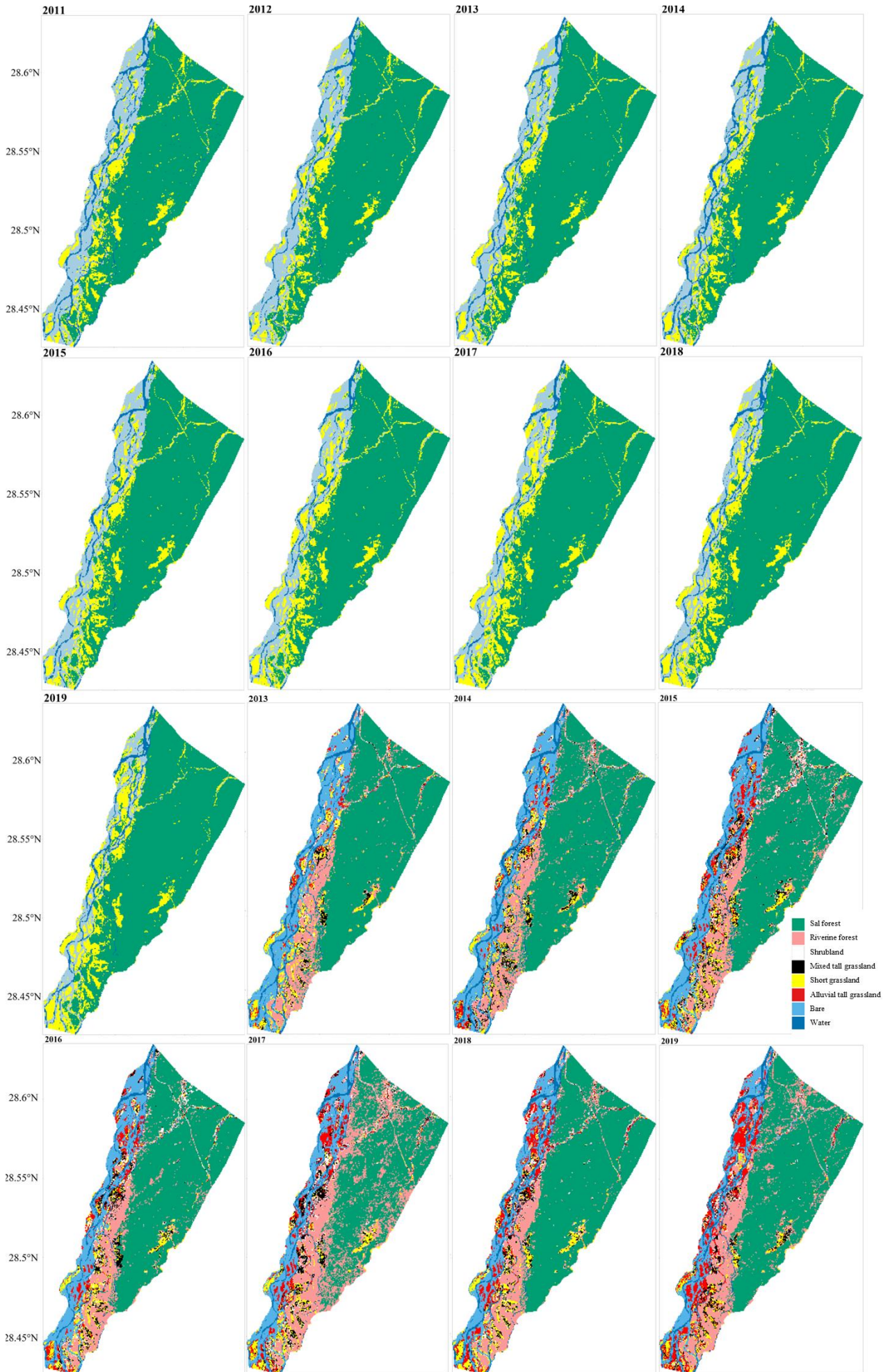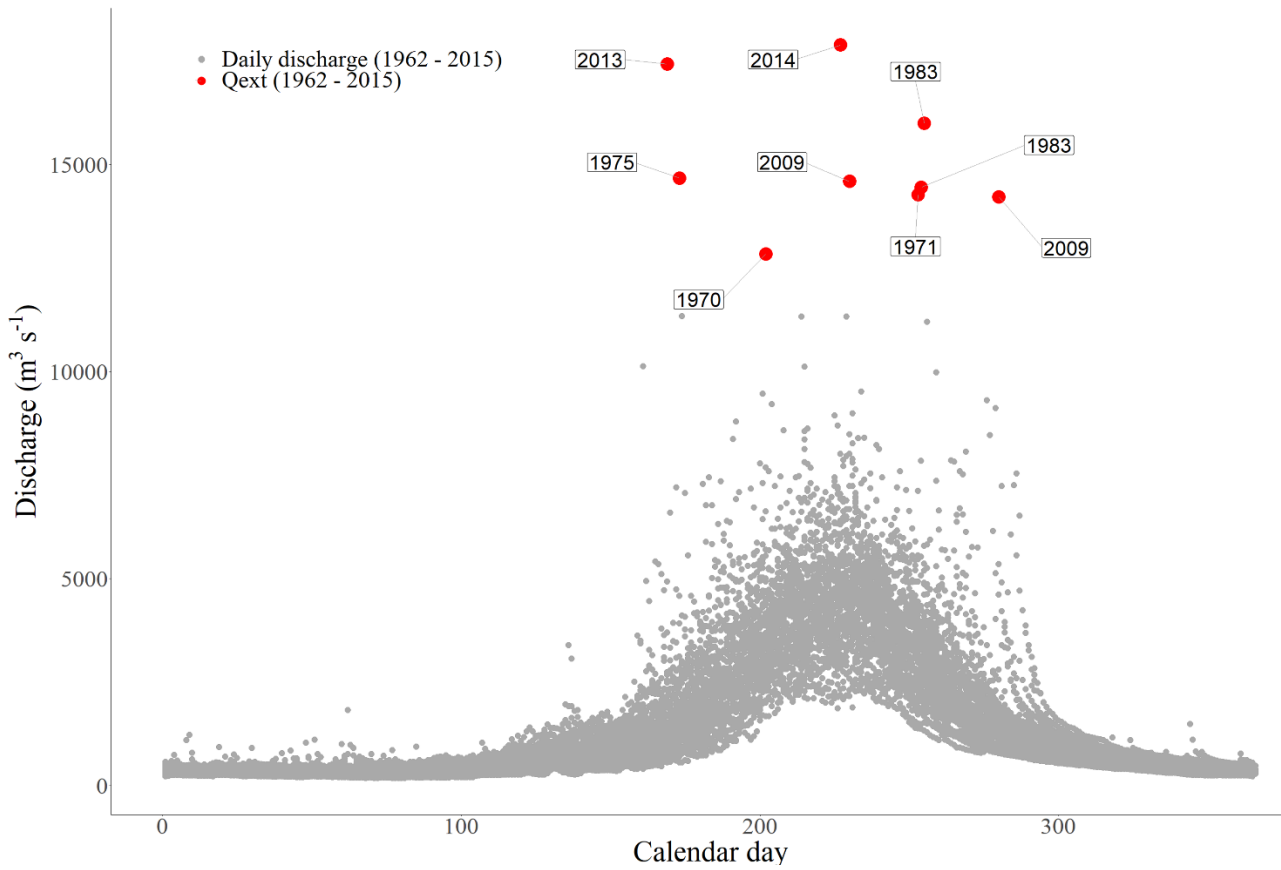
1025 **Figure A4:** Discharge measurements and their calendar day. Red dots represent the identified extreme discharges (Qext) that are larger than 12,500 m3 s-1.

Figure A5: Cattle grazing on the western bank of the Geruwa River along the southwestern border of study area. It demonstrates the grazing
1030 pressure herbivores pose on the vegetation pattern at the border of the park, nowadays, and at earlier times, within the park when cattle grazing was allowed. Photograph taken by authors.